JOC The Journal of Organic Chemistry

Featured Article

pubs.acs.org/joc

Lithium Diisopropylamide-Mediated Ortholithiation of 2-Fluoropyridines: Rates, Mechanisms, and the Role of Autocatalysis

Lekha Gupta, Alexander C. Hoepker, Yun Ma, Mihai S. Viciu, Marc F. Faggin, and David B. Collum*

Department of Chemistry and Chemical Biology, Baker Laboratory, Cornell University, Ithaca, New York 14853-1301, United States

Supporting Information

ABSTRACT: Lithium diisopropylamide (LDA)-mediated ortholithiations of 2-fluoropyridine and 2,6-difluoropyridine in tetrahydrofuran at −78 °C were studied using a combination of IR and NMR spectroscopic and computational methods. Rate studies show that a substrate-assisted deaggregation of LDA dimer occurs parallel to an unprecedented tetramer-based pathway. Standard and competitive isotope effects confirm post-rate-limiting proton transfer. Autocatalysis stems from ArLi-catalyzed deaggregation of LDA proceeding via 2:2 LDA−ArLi mixed tetramers. A hypersensitivity of the ortholithiation rates to traces of LiCl derives from LiCl-catalyzed LDA dimer−monomer exchange and a subsequent monomer-based ortholithiation. Fleeting 2:2 LDA−LiCl mixed tetramers are suggested to be key intermediates. The mechanisms of both the uncatalyzed and catalyzed deaggregations are discussed. A general mechanistic paradigm is delineated to explain a number of seemingly disparate LDA-mediated reactions, all of which occur in tetrahydrofuran at −78 °C.

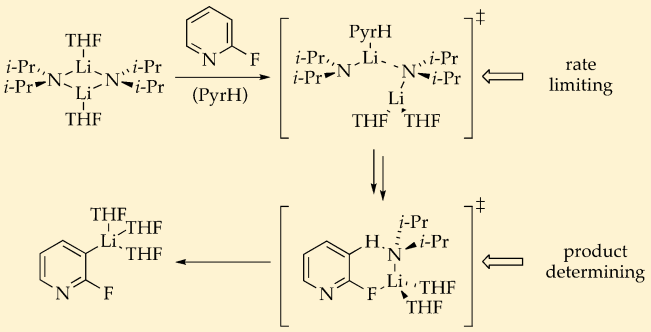

INTRODUCTION

We describe herein mechanistic studies of the lithium diisopropylamide (LDA)-mediated ortholithiation of 2-fluoro- and 2,6-difluoropyridine (eq 1).[1−3] The ortholithiations of **1** and **2** join the ranks of a growing number of LDA-mediated reactions carried out in THF at −78 °C, conditions used routinely by synthetic chemists,[4] in which high substrate reactivities cause aggregation events to become rate limiting.[5,6] Reactions in this emerging class often display virulent autocatalysis, a penchant toward catalysis by added lithium salts (LiCl in particular), and a hypersensitivity to impurities. The mechanistic complexity, a spike in the number of variables that influence the time course of the lithiations, is unlike anything we have detected during studies of organolithium reaction mechanisms that span 25 years.[7] The particular case of fluoropyridine metalation brings two baffling contributions to the developing picture: (1) a substrate-mediated deaggregation of LDA dimer **5** and (2) reaction orders in LDA and catalytically active lithium salts (aryllithium **3** and LiCl) that attest to *associative* aggregation events. Both of these new mechanistic wrinkles are, to date, affiliated only with fluoropyridine metalations.

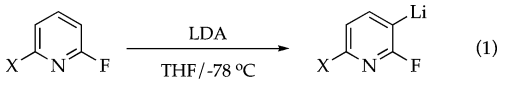

(1)

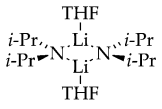

While perusing the paper, those who use LDA routinely should note that commercial samples of LDA behave quite similarly to the analytically pure LDA used in the rate studies below. By contrast, LDA generated in situ from *n*-BuLi and diisopropylamine is equivalent to LDA/LiCl mixtures by manifesting substantially greater reactivity than LiCl-free LDA. The Results section details the protocols and data for specialists. The Discussion section summarizes what we have learned, offers a mechanistic paradigm that covers a number of LDA-mediated reactions, and discusses lingering issues. We begin with background material that is germane to the discussion yet serves as a preface to place the results into context.

Background. During studies of LDA-mediated imine metalations in THF, we noticed that one particularly reactive imine—the only imine for which a reaction temperature of −78 °C is required for monitoring the metalation rate (eq 2)—failed to follow the standard exponential decay, instead showing an oddly linear decay throughout the first two half-lives that was noted but not examined further.[8]

During studies of LDA/THF-mediated ortholithiations of carbamates, the most reactive 3-fluorocarbamate (eq 3)

Received: November 13, 2012
Published: December 27, 2012

   dx.doi.org/10.1021/jo302408r | J. Org. Chem. 2013, 78, 4214−4230

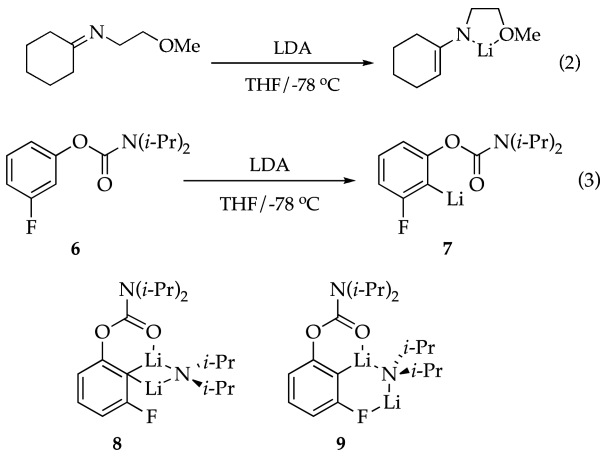

displayed a decidedly linear decay to full conversion (more than five half-lives) that was impossible to ignore.[5a] The linearity, an apparent zeroth-order dependence[9] on **6**, suggested a rate-limiting deaggregation of LDA dimer followed by post-rate-limiting proton transfer. Relatively minor changes in conditions, however, afforded sigmoidal decays implicating significant contributions from autocatalysis.[10] Rate studies showed a first-order rather than a zeroth-order dependence on **6** that did *not* derive from a simple (uncatalyzed) deaggregation of LDA dimer **5**. The linear and sigmoidal decays were traced to an autocatalytic condensation of aryllithium **7** with LDA dimer **5**. Isomeric LDA–ArLi mixed dimers **8** and **9** were shown to react rapidly on the time scales that aggregates exchange. Whether **8** and **9** reacted directly or by facile dissociation remained open to speculation. The metalation was also markedly catalyzed by low concentrations of LiCl (<0.5 mol %).

Subsequent studies of a number of LDA/THF-mediated lithiations of fluorinated arenes at −78 °C revealed strange decays traced to autocatalysis as well as marked LiCl catalysis.[11] For example, LDA/THF-mediated ortholithiation of arene **10** at −78 °C displays a linear decay of **10**, a kinetically controlled formation of regioisomeric aryllithiums **11** and **12**, and a much slower equilibration of **11** and **12** (eq 4).[5c] Rate studies reveal a

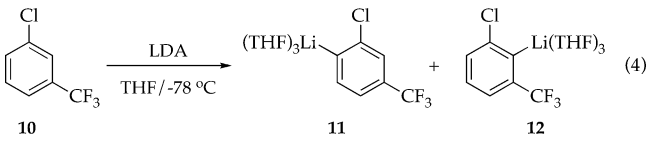

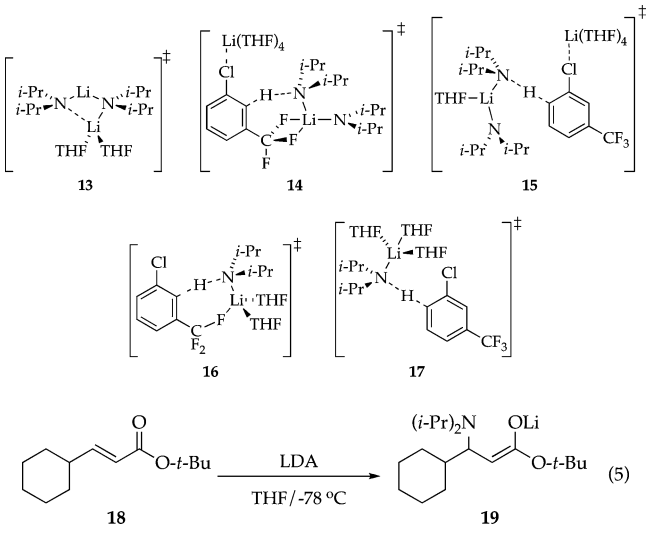

true zeroth-order dependence on **10** with an overlay of autocatalysis. The uncatalyzed deaggregation proceeds via a disolvated dimer; transition structure **13** is supported by density functional theory (DFT) computations. Deuteration shifted the rate-limiting step to deuterium transfer and revealed tetra- and pentasolvated-dimer-based metalations ascribed to triple ions **14** and **15**. Marked acceleration with LiCl was traced to the catalysis of LDA dimer–monomer exchange with a resulting shift in the rate-limiting step from deaggregation to proton transfer. Catalysis allowed us to peer beyond the deaggregation and show that the critical proton transfer proceeds through monomer-based transition structures **16** and **17**.

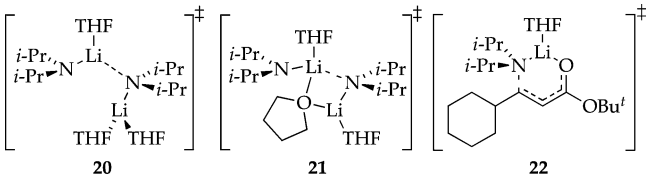

Studies of LDA/THF-mediated 1,4-addition to unsaturated ester **18** at −78 °C (eq 5) revealed a linear loss of substrate, confirming that the strange behavior is restricted to neither ortholithiations nor fluorinated substrates.[5b] In analogy to the ortholithiation in eq 4, the linear decay results from a zeroth-order dependence in substrate arising from a rate-limiting

Scheme 1

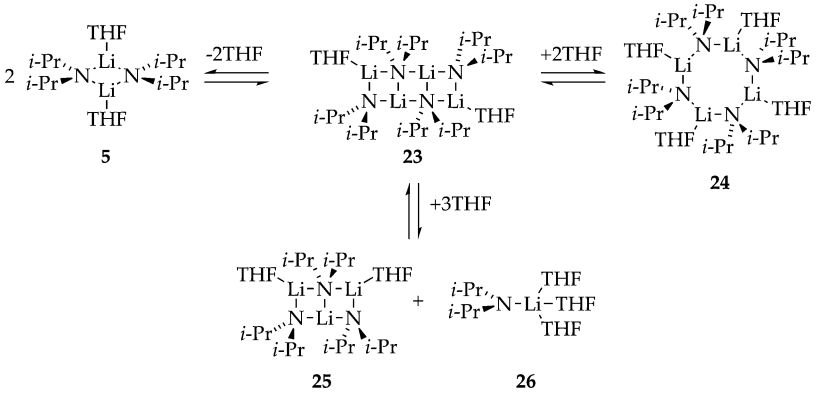

dx.doi.org/10.1021/jo302408r | J. Org. Chem. 2013, 78, 4214–4230

deaggregation of dimer **5**. Notably, the critical deaggregation occurs via a *trisolvated*-dimer-based transition structure, suggested by DFT computations to be trisolvate **20** (or THF-bridged analogue **21**)[5c] rather than disolvate **13**. The existence of two (or more) distinctly different rate-limiting deaggregations is emerging as a central issue. Autocatalysis, although muted because of the low catalytic efficacy of enolates,[5b] elicits counterintuitive rate changes. Once again, LiCl markedly accelerates the reaction by catalyzing dimer−monomer exchange and shifts the rate-limiting step, which allowed us to show that the 1,4-addition proceeds via a monosolvated-monomer-based transition structure, **22**.

Recognizing that aggregation events were *rate limiting* for reactions of LDA in THF at −78 °C, we carried out detailed NMR spectroscopic and DFT computational studies of the dynamic behavior of LDA.[12] NMR spectroscopic studies showed that subunit exchanges (at least nuclear exchanges) occur on approximately the same time scales as the reactions described above (half-life <1 h at 0.10 M LDA in THF at −78 °C). The dominant mechanism of exchange, quite unexpectedly, involved an associative pathway via a *tetrasolvated tetramer*. Computational studies probed the role of ladders (Scheme 1).[13] We could not ascertain, however, whether nuclear exchange involves *symmetrized* cyclic tetramer (**24**) or monomer (**26**). The notion that tetramers are possible sources of monomers has a mechanistic logic that is discussed below.

Computational studies of the apparently slower direct (dissociative) conversion of dimer **5** to monomer **26** revealed a complex series of transformations; the most notable intermediates are shown in Scheme 2.[12] The computed

Scheme 2

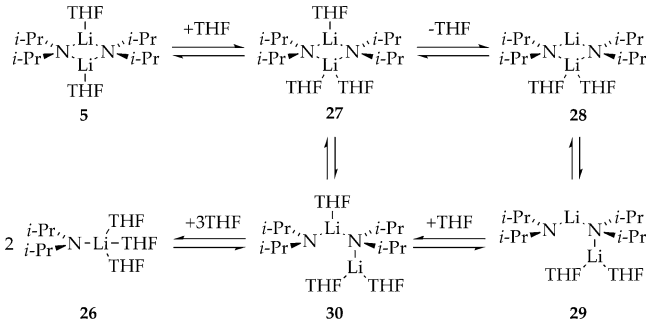

activation barriers for the exchanges in Scheme 2 rise on progression from dimer **5** to monomer **26**. An uncatalyzed, dissociative conversion of dimer **5** to monomer **26** is predicted to involve reversible formation of **27**−**30** and rate-limiting cleavage of **30** via transition structure **20** or **21**. Intermediates **27**−**30**, however, are potentially important intermediates that can be intercepted by substrates (vide infra).

RESULTS

Solution Structures.[14] Structural assignments of LDA and aryllithiums are required to interpret the rate data. Previous studies of [^{6}Li,^{15}N]LDA using ^{6}Li and ^{15}N NMR spectroscopies revealed exclusively disolvated dimer **5**.[15] The ^{13}C NMR spectrum of ArLi **3** shows the lithiated carbon as two 1:1:1 triplets (doublet of triplets) arising from the superposition of ^{6}Li−^{13}C coupling ($^1J_{Li-C}$ = 11.7 Hz) that is split further by especially large ^{13}C−^{19}F coupling ($^2J_{F-C}$ = 124.3 Hz) emblematic of 2-fluoroaryllithiums.[16−18] The ^{19}F{^{1}H}NMR spectrum displays a singlet.[19] Aryllithium **3** in the presence of [^{6}Li,^{15}N]LDA shows no ^{6}Li−^{15}N splitting in **3**, confirming the absence of mixed aggregation.[15] Aryllithium **4** displays spectroscopic properties similar to those of **3** with additional splitting arising from the fluoro moiety at the 6 position. DFT computations of **3** and **4** at the B3LYP/6-31G(d) level[20] with single point calculations at the MP2 level of theory implicate trisolvated monomers (**3a** and **4a**) in accord with other monomeric aryllithiums.[21,22] Numbers **3** and **4** are often used interchangeably with **3a** and **4a** throughout the text, depending on the specific context.

Catalysis by LiCl is discussed in light of the structures of LiCl homoaggregate and LDA−LiCl mixed aggregates. Previous studies showed LiCl to be dimeric (**31**) in THF solution.[7,23] Mixtures of LDA with very low LiCl concentrations (≤2 mol % LiCl) used in the rate studies described below afford a [LiCl]-independent 8:1 mixture of **32** and **33** to the exclusion of free LiCl.[5b,23] Solutions containing [^{6}Li]LiCl and **3a** or **4a** show no evidence of LiCl−ArLi mixed aggregates.

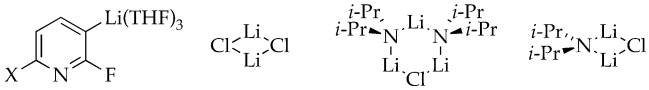

3a; X = H
4a; X = F
31
32
33

Rate Studies. *General Protocols.* We have historically used recrystallized *n*-BuLi[24] to prepare LDA and then recrystallized the resulting LDA.[17] Although potentiometry[25] and ion chromatography[26] have shown that LDA prepared in this manner contains <0.02 mol % LiCl,[5a] the purity proved inadequate for the studies described below because of detectable accelerations elicited by as little as 0.01 mol % LiCl (1 ppm). Accordingly, we prepared LiCl-free LDA from lithium metal and diisopropylamine using a modified[5b] literature protocol[27] and recrystallized the resulting LDA from hexanes, rendering the residual variability acceptable.[28] Anhydrous LiCl was generated in THF solution by lithiation of Et_3N·HCl with LDA.[29] Et_3N is a poor ligand[30] that has no effect on solution structures or reaction rates. Similarly, added diisopropylamine does not influence the ortholithiation.[16]

Reactions were monitored using in situ IR[31] or ^{19}F NMR spectroscopy,[19] the former offering convenience and the latter affording resolution of all ArH and ArLi-related species. Key resonances and absorbances are summarized in Table 1. The choice of method depended on specific needs. In a broader sense, we tactically attempted to study the mechanisms in isolation (under limiting conditions) to the maximum extent possible. Autocatalysis placed an importance on the method of initial rates,[32a] obtained as the first derivative of a polynomial fit

Table 1. IR and ^{19}F NMR Spectroscopic Data

compound	IR absorbance (cm^{-1})	δ ^{19}F^a
1	1598, 1577	−67.8
3	1551, 1517	−40.6
1-d_1		−68.0
2	1613, 1592	−69.0
4	1577, 1515	−44.8, −82.0
2-d_2	1597	−69.2
4-d_1	1499	−82.2, −44.8

^{a}The chemical shifts are reported relative to 0.005 M fluorobenzene in neat THF (−113.15 ppm).

dx.doi.org/10.1021/jo302408r | J. Org. Chem. 2013, 78, 4214−4230

to the raw data at early conversion.[33] Rate laws were routinely assessed using their integral forms. Numeric integrations of the corresponding differential forms included provisions for autocatalysis and other nonlimiting behaviors.

Substrate Dependence. Lithiation of **1** (0.002 M) using LDA (0.10 M[34]) affords a linear decay (Figure 1, curve A).

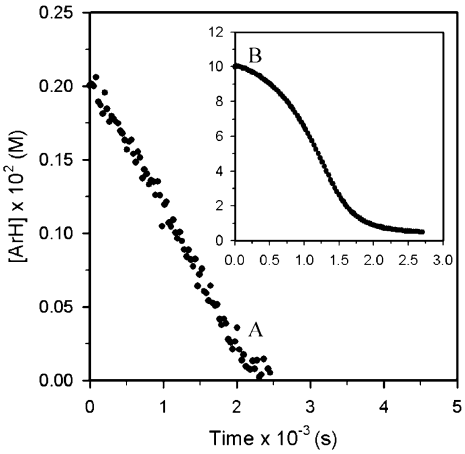

Figure 1. Plot of [**1**] vs time for the ortholithiation of **1** with LDA (0.10 M) in THF (12.20 M) at −78 °C: (A) [**1**] = 0.002 M; (B) [**1**] = 0.10 M.

Increasing the substrate concentration to 0.004 M causes detectable downward curvature, which becomes prominent at elevated substrate concentrations (Figure 1, curve B). Downward (sigmoidal) curvatures are characteristic of autocatalysis.[10] Plotting initial rates, the rates before the onset of autocatalysis, versus substrate concentration (Figure 2) reveals a first-order

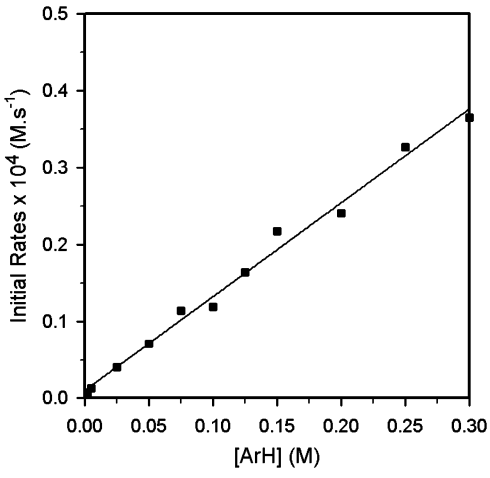

Figure 2. Plot of initial rates vs [**1**] for the ortholithiation of **1** with LDA (0.10 M) in THF (12.20 M) at −78 °C. The curve depicts an unweighted least-squares fit to $-d[\mathbf{1}]/dt = k[\mathrm{ArH}] + k'$ [$k = (1.22 \pm 0.04) \times 10^{-4}$, $k' = (1.0 \pm 0.6) \times 10^{-6}$].

dependence on substrate along with a nonzero *y*-intercept that is either minor or experimental error. Thus, the linear decay at the lowest substrate concentration could arise from (1) the reduction (but not complete elimination) of autocatalysis by the low concentrations of ArLi[35] or (2) a zeroth-order substrate dependence evidenced by the small non-zero intercept. Throughout the remainder of the text, allusions to low and high substrate concentrations (0.002 and 0.10 M, respectively) represent probes of a minor (or nonexistent) substrate-independent pathway and the dominant substrate-dependent pathway, respectively.

THF Dependence. A plot of initial rates versus THF concentration[34] at low substrate concentration (Figure 3, curve

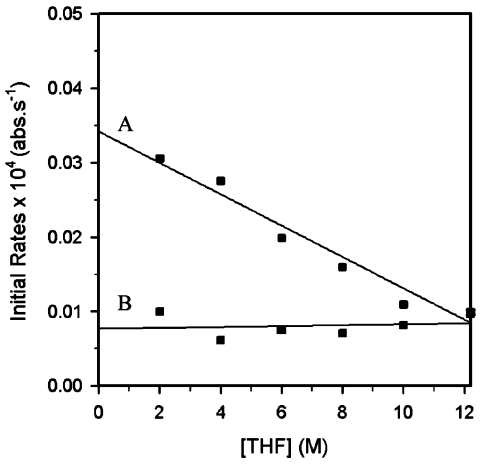

Figure 3. Plot of initial rates vs [THF] for the ortholithiation of **1** (0.002 M) with LDA (0.10 M) at −78 °C. (A) In hexane cosolvent. The curve depicts an unweighted least-squares fit to $-d[\mathbf{1}]/dt = -k[\mathrm{THF}] + k'$ [$k = (2.1 \pm 0.2) \times 10^{-7}$, $k' = (3.4 \pm 0.2) \times 10^{-6}$]. (B) In 2,5-dimethyltetrahydrofuran cosolvent. The curve depicts an unweighted least-squares fit to $-d[\mathbf{1}]/dt = -k[\mathrm{THF}] + k'$ [$k = (6 \pm 19) \times 10^{-9}$, $k' = (8 \pm 1) \times 10^{-7}$].

A) shows an inverse dependence that is oddly linear. (Normal inverse dependencies are hyperbolic.)[7,32a] The inhibition by THF was shown to derive from secondary-shell solvation (medium effects) overlaid on a zeroth-order dependence using a well-tested protocol in which 2,5−dimethyltetrahydrofuran is used as a polar but poorly coordinating cosolvent[36] to maintain a constant polarity of the medium (curve B).

LDA Dependence. Plots of initial rates versus LDA concentration reveal perplexing orders of 1.7 ± 0.3 and 1.5 ± 0.3 at low and high substrate concentrations, respectively (Figure 4). These orders are significantly higher than *any* LDA

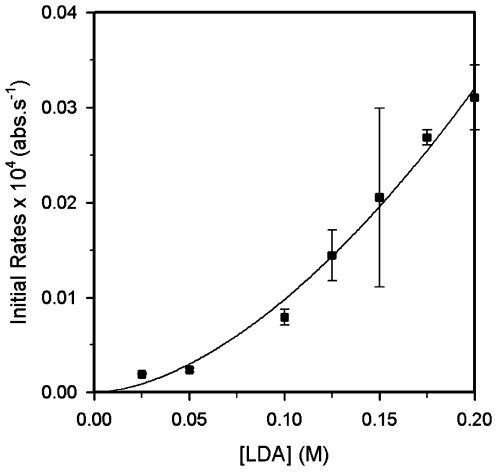

Figure 4. Plot of initial rates vs [LDA] in THF (11.50 M) using hexane as the cosolvent for the ortholithiation of **1** (0.002 M) at −78 °C. The curve depicts an unweighted least-squares fit to $-d[\mathbf{1}]/dt = k[\mathrm{LDA}]^n$ [$k = (5 \pm 2) \times 10^{-5}$, $n = 1.7 \pm 0.3$].

dx.doi.org/10.1021/jo302408r | J. Org. Chem. 2013, 78, 4214−4230

orders measured to date.[7] We cannot exclude the intervention of an uncontrolled variable; the kinetics are extraordinarily sensitive, as reflected by the large error. Nonetheless, any temptation to summarily dismiss the unusual orders is tempered by analogously high LDA orders observed for metalation of difluoropyridine **2** (vide infra) as well as by an order of 1.2 for 3-deutero-2-fluoropyridine, **1**-d_1.

Partial Mechanisms. It is instructive to amalgamate the data described to this point into partial rate laws and mechanisms. Zeroth-order THF dependencies and first-order pyridine dependencies are observed under all conditions. The high, noninteger LDA orders, however, present special challenges that force us to consider several mechanisms and their combinations. We introduce the following shorthand: A = an LDA subunit; S = THF (e.g., A_2S_2 = **5**); ArH = fluoropyridine **1**; and ArLi = aryllithium **3**.

Dimer Mechanism. The most obvious mechanism is the dimer-based pathway described by eqs 6 and 7. Such dimer-based reactions of LDA have been observed on many occasions[7,37] but cannot account for the high LDA orders.

$$-\mathrm{d[ArH]}/\mathrm{d}t = k'[\mathrm{ArH}][\mathrm{A_2S_2}][\mathrm{S}]^0 \quad (6)$$

$$\mathrm{A_2S_2} + \mathrm{ArH} \rightarrow [\mathrm{A_2S_2(ArH)}]^{\ddagger} \quad (7)$$

Trimer Mechanism. A 1.5 LDA order could arise from a dimer−trimer preequilibrium (eqs 8−10). The substrate must participate in the rate-limiting transition structure, although the specific timing of this involvement is unknowable. A dimer−trimer preequilibrium, however, seems to demand the intermediacy of monomers en route to trimers, which is inconsistent with evidence that the lithiation proceeds most efficiently via LDA monomers (vide infra).

$$-\mathrm{d[ArH]}/\mathrm{d}t = k''[\mathrm{ArH}][\mathrm{A_2S_2}]^{1.5}[\mathrm{S}]^0 \quad (8)$$

$$3\mathrm{A_2S_2} \rightleftharpoons 2\mathrm{A_3S_3} \quad (9)$$

$$\mathrm{A_3S_3} + \mathrm{ArH} \rightarrow [\mathrm{A_3S_3(ArH)}]^{\ddagger} \quad (10)$$

Tetramer Mechanism. A tetramer-based reaction (eqs 11 and 12) is without precedent in lithium amides[38,39] but receives support from the dynamic NMR and computational studies showing tetramer-based (associative) LDA exchange (Scheme 1).[12] However, a tetramer-based mechanism cannot, in isolation, account for the high and fractional LDA orders.

$$-\mathrm{d[ArH]}/\mathrm{dt} = k'''[\mathrm{ArH}][\mathrm{A_2S_2}]^2[\mathrm{S}]^0 \quad (11)$$

$$2\mathrm{A_2S_2} + \mathrm{ArH} \rightarrow [\mathrm{A_4S_4(ArH)}]^{\ddagger} \quad (12)$$

Dimer/Tetramer Composite Mechanism. Combinations of the dimer- and tetramer-based mechanisms in parallel are described by eq 13. The composite mechanism includes provisions for any LDA order in the range of 1.0−2.0.

$$-\mathrm{d[ArH]}/\mathrm{d}t = k'[\mathrm{ArH}][\mathrm{A_2S_2}][\mathrm{S}]^0 + k'''[\mathrm{ArH}][\mathrm{A_2S_2}]^2[\mathrm{S}]^0 \quad (13)$$

Isotope Effects. The first-order substrate dependence *appears* to implicate a mechanism(s) that, although disquieting in detail, involves rate-limiting proton transfer. Isotopic labeling studies, however, show that *the critical proton transfer step is post rate limiting.*

The loss of 0.002 M **1**-d_1 versus time displays a substantial upward curvature that contrasts with the linear decay of **1** (Figure 5). Comparing initial rates for **1** and **1**-d_1 measured independently (rather than in direct competition) reveals a

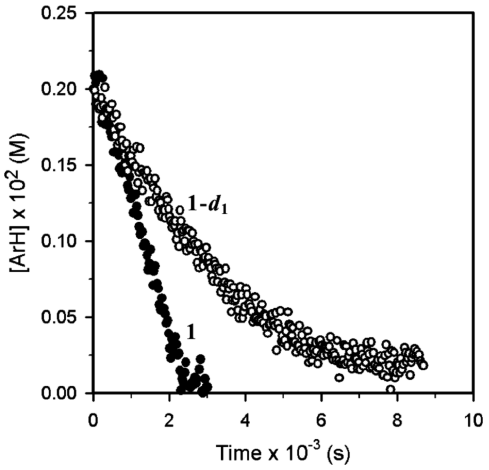

Figure 5. Plot of [ArH] vs time for the ortholithiation of 0.002 M **1** and **1**-d_1 with LDA (0.10 M) in THF (12.20 M) at −78 °C. The metalation of each isotopomer is measured in separate runs (not competitively).

small isotope effect (k_H/k_D = 1.82 ± 0.08). An even smaller value is obtained at high substrate concentrations (k_H/k_D = 1.1 ± 0.3). Metalations of **1** and **1**-d_1 *in competition*, loosely referred to as a competitive isotope effect and discussed extensively below,[40] can be determined from the initial rates by exploiting isotopically sensitive ^{19}F chemical shifts.[41] The resulting isotope effect is large (k_H/k_D = 35 ± 1) but not unusual for such lithiations.[42]

The combination of small standard and large competitive isotope effects offers compelling evidence of a post-rate-limiting proton transfer. This conclusion is supported by following the competition of **1** and **1**-d_1 to full conversion (Figure 6). Arene **1**-d_1 reacts in earnest only after **1** is fully consumed. Such biphasic behavior is observed over a large (0.002−0.10 M) range of substrate concentrations. The curves in Figure 6 result from a best-fit numerical integration to the simplified model in

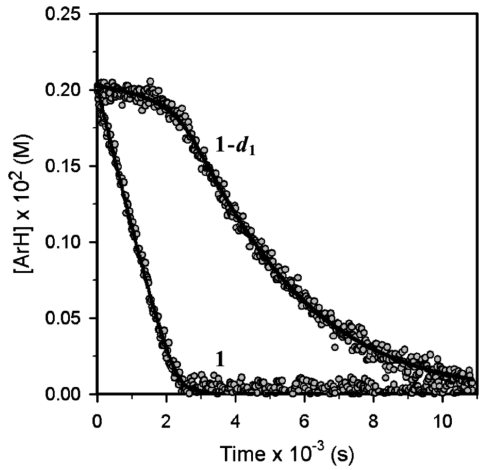

Figure 6. Plot of [ArH] vs time for the ortholithiation of a mixture of fluoropyridines **1** and **1**-d_1 (0.002 M each) with LDA (0.10 M) in THF (12.20 M) at −78 °C, monitored by ^{19}F NMR spectroscopy. The curves result from a best-fit numerical integration to the model in Scheme 3 (Supporting Information).

dx.doi.org/10.1021/jo302408r | J. Org. Chem. 2013, 78, 4214−4230

Scheme 3. (A model in which the key intermediate is an activated dimer, A_2*, rather than two monomers fits equally well.)

Scheme 3

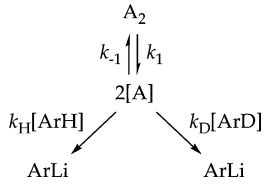

Two additional observations are subtle but important. First, the large competitive isotope effect *requires* that facile ArH/ArD ligand exchange occurs on the fleeting deaggregated form of LDA (monomer A in Scheme 3, for example) *before* the post-rate-limiting proton transfer. Second, the small but measurable standard isotope effect and upward curvature arising from **1**–d_1 (Figure 5, curve B) indicate that deuterium transfer is *partially* rate limiting, which is supported by the fit in Figure 6 showing a 20:1 ratio of the forward to reverse reaction rates (k_D[ArD]-[A]/k_{-1}[A]^2 = 20).

Ligand Catalysis. The combination of a substrate dependence, a post-rate-limiting proton transfer, and a large competitive isotope effect suggested that we might be able to catalyze the metalation of **1** with a catalyst bearing some of the structural attributes of **1**. We attempted to mimic substrate-catalyzed deaggregation with a variety of added ligands, including pyridine (**34**), fluorobenzene (**35**), and silylated fluoropyridine **36**; none detectably catalyzed the metalation of **1**. Curiously, 6–silylpyridine **37** metalates nearly as efficiently as **1** despite the hindrance about the nitrogen, and it appears to be susceptible to the same substrate-dependent deaggregation. Catalysis of deaggregation is a recurring theme in subsequent sections.

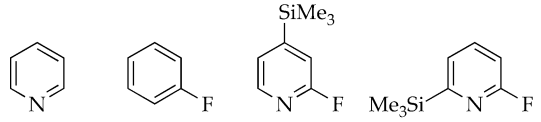

34 **35** **36** **37**

LiCl Catalysis. Traces of LiCl elicit marked rate accelerations accompanied by distinct upward curvatures (Figure 7). First-order decays are observed at >0.3 mol % LiCl. A plot of the initial rates versus LiCl concentration shows saturation kinetics (Figure 8). Sigmoidal curvature evident at the low LiCl concentrations signifies a high (approximately second) order in LiCl.

Seemingly analogous LiCl saturation behavior (absent the sigmoid) is observed for ortholithiations of arene **10** (eq 4) and 1,4-additions of LDA to unsaturated esters (eq 5). The saturation behavior is *not* Michaelis–Menten kinetics, which would require stoichiometric LiCl to attain saturation. The saturation behaviors were traced instead to LiCl-catalyzed deaggregation of LDA accompanied by a shift in the rate-limiting step as follows.[5b,c]

Monitoring the ortholithiation of **1** at full saturation (2 mol % LiCl) reveals large standard and competitive isotope effects (k_H/k_D = 33 and 23, respectively), showing that LiCl catalysis causes proton transfer to become rate limiting. Importantly, the catalysis offers a view beyond what had been a rate-limiting

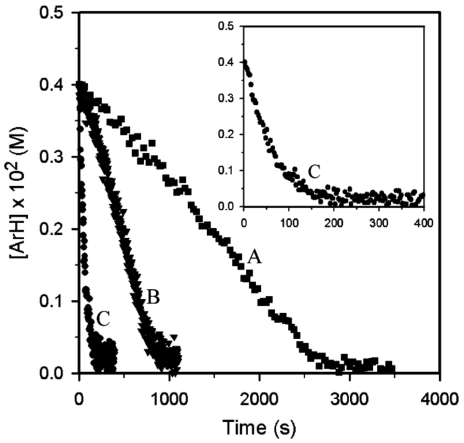

Figure 7. Plot of [**1**] vs time for the ortholithiation of **1** (0.004 M) with LDA (0.10 M) in 12.20 M THF at −78 °C in the presence of varying mol percentages of LiCl: (A) no LiCl; (B) 0.05 mol % LiCl; (C) 0.6 mol % LiCl.

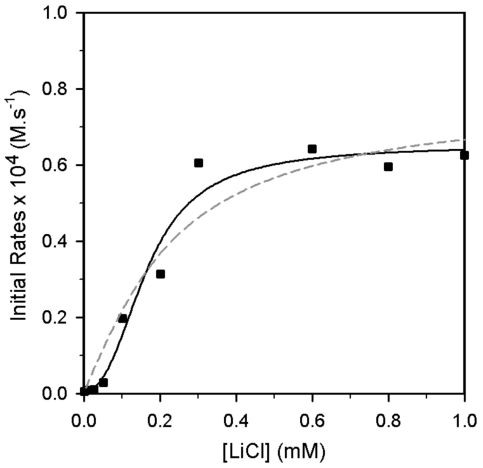

Figure 8. Plot of initial rates vs [LiCl] for the ortholithiation of **1** (0.004 M) with LDA (0.10 M) in THF (12.20 M) at −78 °C. The solid curve depicts an unweighted least-squares fit to eq 16. See the Supporting Information for derivation. [c = (5 ± 1) × 10^{-7}, n = 2 (fixed), and k_1 = (1.6 ± 0.1) × 10^{-2}, k_{-1} = (1.03 ± 0.03) × 10^4, k_2 = (5.901 ± 0.002) × 10^1.] The dashed curve represents a fit to the data where n = 1 in the given equation.

deaggregation. Plotting k_{obsd} versus LDA concentration (Figure 9) affords a generic half-order dependence implicating a dimer–monomer preequilibrium and monomer-based metalation. A plot of k_{obsd} versus THF concentration (Figure 10) shows an ambiguous dependence that could be interpreted as either (1) a first-order dependence with a single renegade point at the highest THF concentration (solid curve) or (2) a second-order dependence with a nonzero intercept (dashed curve). Although the former seems most palatable by inspection, the latter is supported by the analogous plot using **1**-d_1, which shows a more distinct upward curvature (Figure 10, inset) and a nonzero intercept. Thus, we remain agnostic on the solvation number at the rate-limiting transition structure and present the mechanism according to eqs 14–17. The rate law in eq 16 includes provisions for second-order saturation by LiCl (Figure 8). The odd mathematical form of eq 16 stems from the solution to the quadratic equation required by the dimer–monomer preequilibrium.[21] In the limit of full

dx.doi.org/10.1021/jo302408r | J. Org. Chem. 2013, 78, 4214–4230

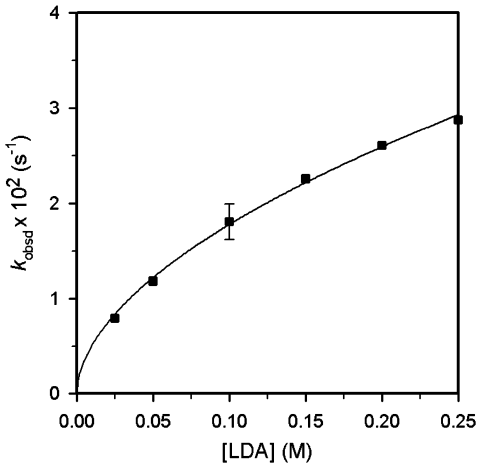

Figure 9. Plot of k_{obsd} vs [LDA] for the ortholithiation of **1** (0.004 M) in 12.20 M THF in the presence of 2 mol % of LiCl at −78 °C. The curve depicts an unweighted least-squares fit to $k_{obsd} = k[\mathrm{LDA}]^n$ [k = (6.2 ± 0.4) × 10^{-2}, n = (0.54 ± 0.03).].

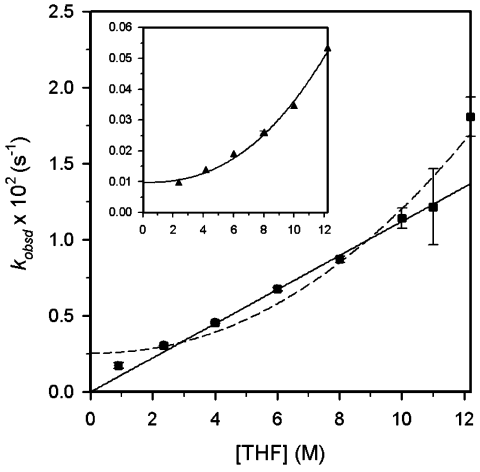

Figure 10. Plot of k_{obsd} vs [THF] in hexane cosolvent for the ortholithiation of **1** (0.004 M) with LDA (0.10 M) in the presence of 2 mol % LiCl at −78 °C. The solid line depicts an unweighted least-squares fit to $k_{obsd} = k[\mathrm{THF}]$, with the point at 12.2 M THF excluded (k = (1.12 ± 0.03) × 10^{-3}). The dashed curve depicts an unweighted least-squares fit to $k_{obsd} = k[\mathrm{THF}]^n + k'$ [k = (8 ± 7) × 10^{-5}, n = (2.0 ± 0.4), k' = (2.5 ± 0.7) × 10^{-3}]. Inset shows the corresponding plot for the ortholithiation of **1**-d_1 (0.004 M). The curve depicts an unweighted least-squares fit to $k_{obsd} = k[\mathrm{THF}]^n + k'$ [k = (1.1 ± 0.6) × 10^{-6}, n = (2.4 ± 0.2), k' = (10 ± 1) × 10^{-5}].

saturation (>0.3 mol % LiCl), eq 16 reduces to eq 17 as described in detail previously.[5b]

$$A_2S_2 + 2m\mathrm{THF} \underset{k_{-1}[\mathrm{LiCl_{total}}]^n}{\overset{k_1[\mathrm{LiCl_{total}}]^n}{\rightleftharpoons}} 2AS_{m+1} \quad (14)$$

$$AS_{m+1} + \mathrm{ArH} \overset{k_2}{\rightarrow} [AS_{m+1}(\mathrm{ArH})] \quad (15)$$

$$-\Delta[\mathrm{ArH}]/\Delta t|_{t=0} = \frac{k_2[\mathrm{ArH}]}{4k_{-1}[\mathrm{LiCl}]^n} \times (\sqrt{k_2^2[\mathrm{ArH}]^2 + 16k_1k_{-1}[A_2S_2][\mathrm{LiCl}]^{2n}[\mathrm{THF}]^{2m}} - k_2[\mathrm{ArH}]) + c \quad (16)$$

$$-\Delta[\mathrm{ArH}]/\Delta t|_{t=0} = (k_1/k_{-1})^{1/2}k_2[\mathrm{ArH}][\mathrm{THF}]^{2m}[\mathrm{LDA}]^{0.5} \quad (17)$$

A highly attenuated saturation behavior is observed for LiCl-catalyzed lithiations of **1**-d_1 (Supporting Information). The barely discernible catalysis supports the previous assertion that deuteration renders the proton transfer partially rate limiting.

Mechanisms. With LiCl catalysis facilitating monomer-based metalation of somewhat ambiguous solvation number, we turned to DFT computations to fill in elusive details. Mono-, di-, and trisolvated monomer-based transition structures **38**−**40** all may be viable; the disolvate is suggested to be the preferred form. Li−F interactions appear to be mechanistically important as noted in previous studies.[5a,43,44] Intrinsic reaction coordinate (IRC) calculations focusing on the computationally most viable disolvate **39** show that it is preceded and succeeded by minima corresponding to **41** and **42**, respectively (eq 18).

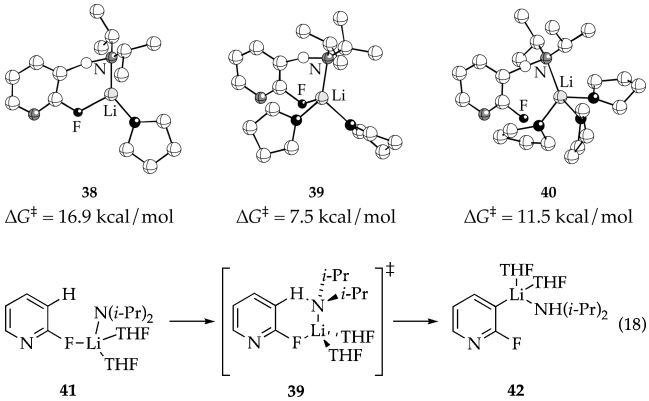

Autocatalysis. Equations 6−13 describe possible rate-limiting deaggregations that could be prevalent at early conversion. By contrast, eqs 14, 15, and 17 describe lithiation under conditions of a fully established dimer−monomer equilibrium (LiCl catalyzed). We can now consider the autocatalysis evident in Figure 1 (curve B). Recall that no *observable* mixed aggregates are formed from LDA and aryllithium **3**.

A standard control experiment that we routinely use to show the *absence* of autocatalysis under pseudo-first-order conditions is carried out by zeroing the IR baseline at the end of a kinetic run and measuring a rate constant from adding a second aliquot of substrate. The second rate constant should be indistinguishable from the first except for a very small reduction in rate resulting from loss of LDA titer. Instead, we noted a rate *increase* from a second aliquot of **1**, suggesting that aryllithium **3** accelerates the reaction. The impact of autocatalysis is readily discerned by incrementally adding arene **1** to a solution of LDA and monitoring the initial rates. Overall, a molar equivalent of substrate is added in small aliquots, which minimizes the influence of substrate-catalyzed deaggregation. The first notable observation is that the presence of ArLi elicits upward curvatures in the decay of ArH, suggesting that ArLi-derived catalysis at least partially shifts the rate-limiting step from LDA deaggregation to a reaction in which substrate **1** participates. A plot of the initial rates versus the mole fraction of aryllithium **3** (X_{ArLi}) is illustrated in Figure 11. The positive deviation from the dotted curve (visible just above the X-axis) represents the contribution of autocatalysis. This variant of a Job plot[45,46] detects even low levels of autocatalysis that could be concealed in decays that are already distorted by rate-limiting deaggregation. The maximum in the curve corresponding to 1:1 ArLi:LDA titer (normality *not* molarity) shows the optimum stoichiometry to be equal proportions of ArLi and

dx.doi.org/10.1021/jo302408r | J. Org. Chem. 2013, 78, 4214−4230

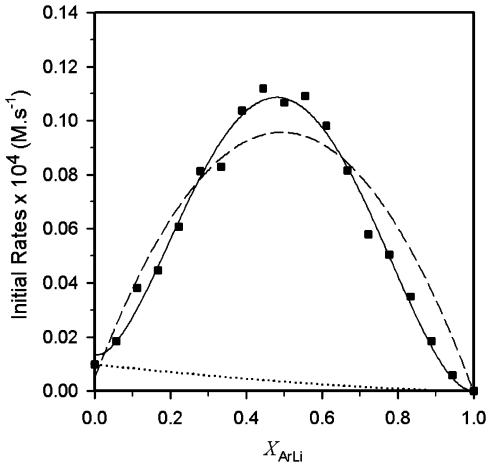

Figure 11. Plot of initial rates versus mole fraction of 3-lithio-2-fluoropyridine (X_{ArLi}) for the serial injections of 0.0055 M aliquots of **1** to 0.10 M LDA in 12.20 M THF at −78 °C. The dotted line depicts the theoretical initial rates in the absence of autocatalysis, assuming an LDA order of 1.5. The solid curve depicts an unweighted least-squares fit to eq 19. See the Supporting Information for the derivation. [m = 1.9 ± 0.1, n = 1.9 ± 0.1, k = (1.5 ± 0.3) × 10^{-4}, k' = (1.3 ± 0.4) × 10^{-6}.] The dashed curve represents a fit to the data where m = 1 and n = 1.

LDA subunits, $[(i\text{-Pr})_2\text{NLi}]_m(\text{ArLi})_n$ ($m = n$). The fit to $m = n = 1$ (dashed curve in Figure 11), however, is obviously inadequate. A nonlinear least-squares fit to eq 19[21] to ascertain the order (solid curve in Figure 11) is excellent and implicates a mixed tetramer, $[(i\text{-Pr})_2\text{NLi}]_m(\text{ArLi})_n$ (m = 1.9 ± 0.1; n = 1.9 ± 0.1).[45d]

$$-\Delta[\text{ArH}]/\Delta t = k(\text{X}_{\text{ArLi}})^n(1 - \text{X}_{\text{ArLi}})^m + k'(1 - \text{X}_{\text{ArLi}})^{1.5} \quad (19)$$

We monitored initial rates versus ArLi concentration at constant LDA concentration (Figure 12), revealing saturation behavior akin to that observed for LiCl (Figure 8). A nonlinear least-squares fit with the ArLi order as an adjustable parameter

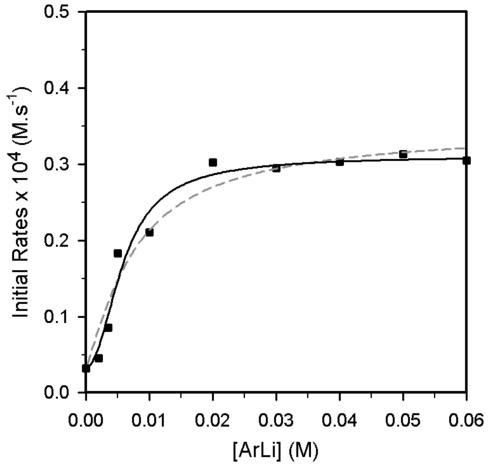

Figure 12. Plot of initial rates vs [ArLi] for the ortholithiation of **1** (0.005 M) with LDA (0.10 M) in THF (12.20 M) at −78 °C. The curve depicts an unweighted least-squares fit to eq 16, where LiCl is substituted for ArLi. See the Supporting Information for derivation. [c = (3.2 ± 0.5) × 10^{-6} and n = 1.7 ± 0.4, k_1 = 1.2 ± 2.6, k_{-1} = (1.6 ± 0.2) × 10^3, k_2 = (9.2 ± 11.5) × 10^{-1}.] The dashed curve represents a fit to the data where n = 1.

reveals a best-fit order of 1.7 ± 0.4, supporting the putative high-order dependence on ArLi. Rate studies at full saturation (≥0.03 M ArLi) reveal a half-order dependence on LDA, confirming the dominance of the same monomer-based metalation(s) as that observed under LiCl catalysis.

Evidence of a mixed tetramer-based autocatalysis (eqs 20 and 21) in conjunction with the data in Figure 11 allowed us to calculate the relative contribution of the uncatalyzed and autocatalyzed pathways versus percent conversion assuming reaction of equimolar LDA and pyridine **1** (Figure 13).

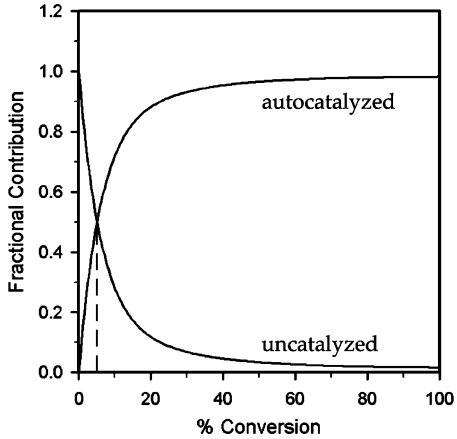

Figure 13. Plot of fractional contribution of the autocatalyzed and uncatalyzed pathway to the total reaction rates vs percent conversion derived from the data in Figure 11. Equal contribution from the two pathways (dashed line) occurs at 6% conversion.

Although the catalytic efficiency of ArLi pales compared to that of LiCl, autocatalyzed deaggregation is dominant at >6% conversion.

$$-\Delta[\text{ArH}]/\Delta t = k_{\text{cat}}[\text{ArLi}]^2[\text{A}_2] \quad (20)$$

$$\text{A}_2 + 2\text{ArLi} \xrightarrow{k_{\text{cat}}} [\text{A}_2(\text{ArLi})_2] \xrightarrow{2\text{ArH}} 4\text{ArLi} \quad (21)$$

*2,6-Difluoropyridine (**2**).* Extensive data was amassed on the ortholithiation of difluoropyridine **2**. Because of significant parallels with **1**—even the odd LDA orders were detected—the data have been relegated largely to the Supporting Information. Several differences, however, are notable:

(i) The metalation of **2** is decidedly less susceptible to autocatalysis than is the metalation of **1**, which could stem from either a muted susceptibility of the metalation to catalysis or a muted activity of aryllithium **4** as a catalyst. Control experiments involving added mono- and difluoroaryllithiums **3** or **4** to metalations of arenes **1** or **2** show that the differences stem from a low catalytic activity of aryllithium **4**.

(ii) Plots of initial rate versus concentration of **2** show a first-order dependence analogous to that in Figure 2 but with a 7-fold greater slope than for **1**. We caution that the higher metalation rate can *not* be attributed to increased acidity at least in a simple sense because the proton transfer is post rate limiting. The higher reactivity of **2** relative to **1** stems from a more efficient substrate-mediated deaggregation. Competition of **1** and **2** shows biphasic kinetics consistent with a post-rate-limiting proton transfer (Figure 14). The 7-fold greater metalation rate for **2** when measured separately and the 30-fold greater rate when measured in competition of **1** and **2**

dx.doi.org/10.1021/jo302408r | J. Org. Chem. 2013, 78, 4214−4230

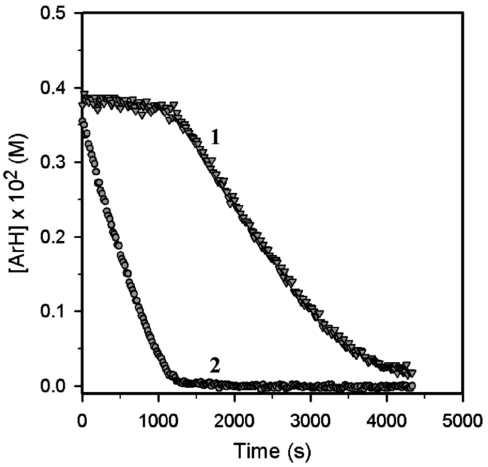

Figure 14. Plot of [ArH] vs time for the ortholithiation of a mixture of fluoropyridines **1** and **2** (0.004 M each) with LDA (0.10 M) in THF (12.20 M) at −78 °C, monitored by ^{19}F NMR spectroscopy.

suggest that the substrate properties influencing deaggregation differ from those that influence the proton transfer.

(iii) Small standard isotope effects in conjunction with large competitive isotope effects and biphasic kinetics (analogous to those illustrated in Figure 6) confirm a post-rate-limiting proton transfer at low substrate concentration. At high substrate concentration, however, an intermediate standard isotope effect (k_H/k_D = 14) suggests that deuterium transfer is substantially rate limiting.

(iv) Pronounced LiCl catalysis causes the rates to become immeasurably fast at concentrations that might have afforded saturation behavior. In contrast to the greater catalytic efficiency of **2** compared to **1** (described in part ii above), the higher reactivity of **2** versus **1** under LiCl catalysis is due to the 30-fold greater kinetic acidity of **2**. A second-order dependence on LiCl for pyridine **2** (Figure 15) supports the second-order saturation behavior of pyridine **1** (Figure 8).

DISCUSSION

Mechanistic studies of the LDA-mediated ortholithiation of 2-fluoropyridine (**1**) afforded results that are surprising, in some cases unprecedented, and at times seemingly paradoxical. The complexity stems from several factors: (i) a rate-limiting deaggregation mediated by fluoropyridine **1**, (ii) evidence of tetramer and mixed tetramer-based deaggregations, (iii) changes in the rate limiting step with minor changes in reaction conditions, (iv) autocatalysis by aryllithium **3**, and (v) highly efficient catalysis by LiCl. There is a natural tension between our need as authors to compartmentalize the variables for presentation and the inherent correlations of these variables. Additional pedagogic challenges arise from comparisons of fluoropyridine metalations with the LDA/THF-mediated reactions summarized in the background section that, although mechanistically related, can display strikingly different behaviors.

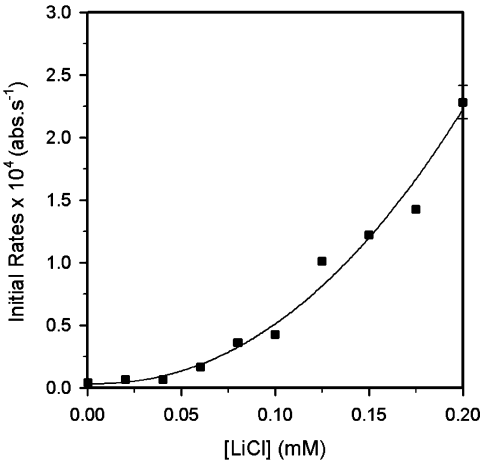

Figure 15. Plot of initial rates vs [LiCl] for the ortholithiation of **2** (0.004 M) with LDA (0.10 M) in THF (12.20 M) at −78 °C. The curve depicts an unweighted least-squares fit to $-d[\mathbf{2}]/dt = k[\mathrm{LiCl}]^n + k'$ [$k = (7 \pm 3) \times 10^{-3}$, $n = 2.2 \pm 0.3$, $k' = (3 \pm 7) \times 10^{-6}$].

Overview. We begin the discussion by painting a picture of the mechanism using the broadest of brush strokes with details provided in subsequent sections. The sum of our efforts described by Scheme 4 illustrate the three important phases of an ortholithiation—deaggregation, complexation, and proton transfer. We took the liberty in the Results to introduce a shorthand: A = an LDA subunit; S = THF, ArH = fluoropyridine **1**, and ArLi = aryllithium **3**.

Scheme 4

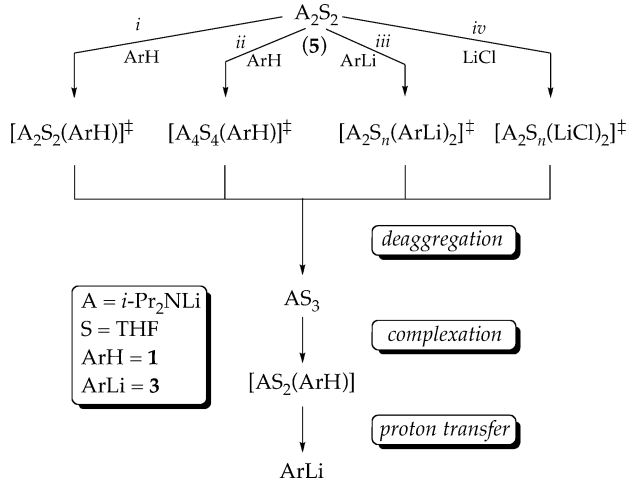

Monitoring the lithiation of pyridine **1** at early conversion, before the onset of autocatalysis, reveals evidence of parallel pathways involving disolvated dimers and tetrasolvated tetramers (Scheme 4, pathways *i* and *ii*.) Although both display seemingly generic first-order substrate dependencies, isotopic labeling studies show that the proton transfers occur *subsequent* to rate-limiting deaggregation(s). We offer transition structures **43**−**47** as possible transition structures. Dimer-based structures **43** and **44** are well founded in detailed computational studies of LDA deaggregation.[12] Preliminary studies show that **45**−**47** are credible as well. Such tetramer-based deaggregations appear only sporadically (vide infra).

As the metalation proceeds to full conversion, reaction of aryllithium **3** with LDA dimer **5** elicits autocatalysis (Scheme 4, pathway *iii*) traced to ArLi-catalyzed deaggregation of LDA dimer **5** to monomer **26** (Scheme 5). Computational studies added support and structural detail to **39**. Rate studies implicate fleeting 2:2 mixed tetramers, [A$_2$(ArLi)$_2$] (vide infra). Autocatalysis is accompanied by a shift of the rate limiting step to monomer-based metalation via transition structure **39**.

dx.doi.org/10.1021/jo302408r | J. Org. Chem. 2013, 78, 4214−4230

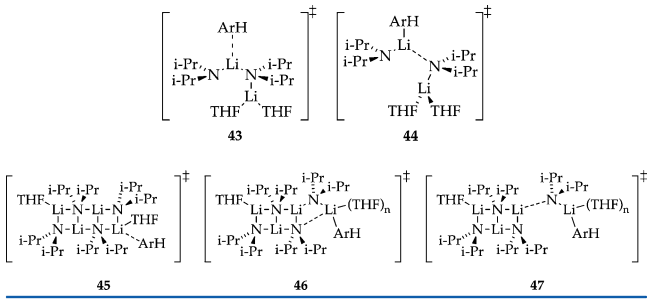

Scheme 5

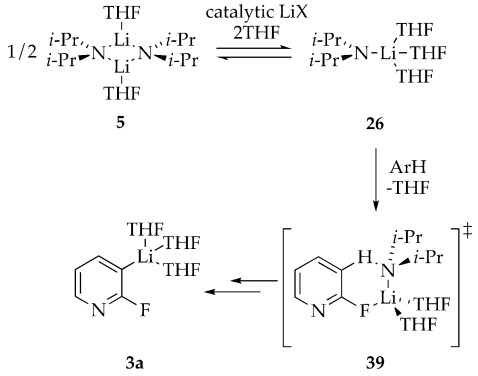

Autocatalysis foreshadowed accelerations by LiCl (Scheme 4, pathway *iv*). Catalysis by as little as 0.001 mol % of LiCl wreaked havoc on the rate studies until rigorously LiCl-free LDA was prepared.[5b] Rate studies show once again that catalysis of dimer−monomer exchange is accompanied by a shift in the rate-limiting step from deaggregation to proton transfer (transition structure **39**; Scheme 5). Lithium chloride, however, is a far more efficient catalyst than is aryllithium **3a**. The shift in the rate-limiting step allowed us to investigate the monomer-based proton transfer occurring beyond the formerly rate-limiting deaggregation.

Aside from the obvious omission of a few details, this summary paints a complex but seemingly coherent picture of LDA-mediated lithiation of fluoropyridine **1**. There are nuances, however, that are quite perplexing as discussed below.

Role of Rate-Limiting Steps: A Mechanistic Paradigm. In this section, we describe a mechanistic paradigm that has been developing over a series of studies,[5,11,12] a paradigm that includes provisions for a seemingly disparate collection of observations all revolving around rate-limiting deaggregation or substrate complexation. The approach may seem overly methodical, but it is imperative that the reader understand the determinants of rate limitation. With the nonspecialist in mind, we begin from first principles using the simplest possible model (eq 22).

$$\mathrm{SM} \underset{k_{-1}}{\overset{k_1}{\rightleftharpoons}} [\mathrm{I}] \overset{k_2}{\rightarrow} \mathrm{P} \qquad (22)$$

Assume that intermediate, I, is relatively unstable ($k_{-1} \gg k_1$). The rate-limiting step of the overall conversion of starting material, SM, to product, P, is determined by the fate of I. If $k_2 \ll k_{-1}$, then I will return to SM with high fidelity, only occasionally giving P; conversion of I to P is rate limiting. By contrast, if $k_2 \gg k_{-1}$, then I always affords P; conversion of SM to I is rate limiting. Thus, it is the k_2/k_{-1} ratio, the penchant of I to give product or return to starting material, that dictates rate limitation. This is an important concept that we will rely on heavily in the forthcoming discussion.

To understand the role of catalysis and autocatalysis, let us assume that $k_2/k_{-1} \gg 1$ (formation of I is rate limiting) and introduce a catalyst to facilitate the conversion of SM to I. Using a minor short cut, catalysis can be thought of as simply increasing k_1,[47] which will afford higher reaction rates. Less obvious, perhaps, is that the reverse reaction of I to SM is necessarily accelerated proportionately—think of a proportionate increase in k_{-1}—as mandated by the principle of microscopic reversibility.[48] At some elevated level of catalysis, the catalyzed back reaction becomes so efficient that I returns to SM faster than it reacts to give P ($k_2/k_{-1} \ll 1$); conversion of I to P becomes rate limiting. Thus, catalyzing the conversion of SM to I (the forward reaction) causes the acceleration, whereas catalyzing I to SM (the back reaction) causes the shift in the rate-limiting step.

Now we can bring elements of organolithium chemistry to the model. Scheme 6 depicts a monomer-based metalation that is simple but not overly simplified. Monomer **48** is arbitrarily drawn with only two solvents, although the resting state is more likely trisolvate **26**, which is unimportant. What *is* important is that by considering three limiting behaviors of this simple mechanism we can begin to understand the consequences and nuances of rate limitation. A summary of the predicted behaviors is included in Table 2.

Case 1: Rate-Limiting Proton Transfer. Under most circumstances, circumstances that have dominated our rate studies of LDA-mediated metalations for 25 years,[7] the proton transfer described by k_3 is rate limiting. Fleeting intermediates **48** and **49** are formed reversibly. Complex **49** has a much greater probability of returning to dimer **5** than forming aryllithium **50**. In short, $k_3[\mathbf{49}] \ll k_{-2}[\mathbf{49}]$ and $k_{-1}[\mathbf{48}]$.[2] The equilibrium approximation[32] affords a rate law showing first-order dependencies on both substrate and THF concentrations (eq 23). The half-order dependence on LDA concentration is a consequence of the dimer−monomer preequilibrium.[7] Comparing ArH and ArD would reveal a large standard isotope effect (typically $k_H/k_D > 7$, but it can exceed 30).[49] Competition of ArH and ArD in the same vessel would afford what we loosely refer to as a competitive isotope effect[41] that is comparable to the standard isotope effect, confirming that the isotopically sensitive proton transfer is also rate limiting.

$$\mathrm{d[ArLi]/d}t = k'[\mathrm{ArH}][\mathrm{LDA}]^{1/2}[\mathrm{THF}] \qquad (23)$$

Scheme 6

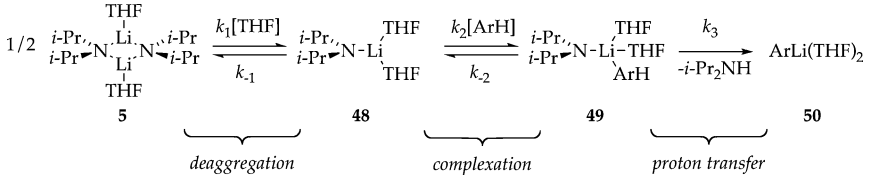

dx.doi.org/10.1021/jo302408r | J. Org. Chem. 2013, 78, 4214−4230

Table 2. Summary of Plausible Mechanisms for LDA-Mediated Reactions

case	rate-limiting step	relative rates	rate law d[ArLi]/dt	standard isotope effect (k_H/k_D)	competitive isotope effect (k_H/k_D)
1	proton transfer	$k_3[\mathbf{49}] \ll k_{-2}[\mathbf{49}]$ and $k_{-1}[\mathbf{48}]^2$	$k'[\mathrm{ArH}][\mathrm{LDA}]^{1/2}[\mathrm{THF}]$	large	large
2	complexation	$k_{-2} \ll k_3$	$k'[\mathrm{ArH}][\mathrm{LDA}]^{1/2}[\mathrm{THF}]$	1	1
2	complexation *(facile ArH–ArD exchange)*	$k_{-2} \ll k_3$	$k'[\mathrm{ArH}][\mathrm{LDA}]^{1/2}[\mathrm{THF}]$	1	large
3	deaggregation	$k_{-1}[\mathbf{48}]^2 \ll k_2[\mathrm{ArH}][\mathbf{48}]$ and $k_3[\mathbf{49}]$	$k'[\mathrm{LDA}]^1[\mathrm{THF}]^n$	1	large
4	partial rate-limiting proton transfer	$k_{-1}[\mathbf{48}]^2 \approx k_3[\mathbf{49}]$	$k'[\mathrm{ArH}]^{0-1}[\mathrm{LDA}]^{1/2-1}[\mathrm{THF}]^n$	>1	>1

Case 2: Rate-Limiting Complexation. In case 2, we assume the proton transfer is fast. This is likely to occur with particularly acidic substrates. By coincidence, these substrates are those that undergo LDA/THF-mediated reactions within a few degrees of −78 °C. Under these synthetically prominent conditions, aggregation events occur on minute rather than microsecond time scales.[12] In this limiting case, **5** deaggregates to give **48** reversibly, and complexation to form **49** is rate limiting ($k_{-2} \ll k_3$). There are two possible outcomes, depending on whether a post-rate-limiting exchange of ArH and ArD occurs before proton transfer (Scheme 7). In the first

Scheme 7

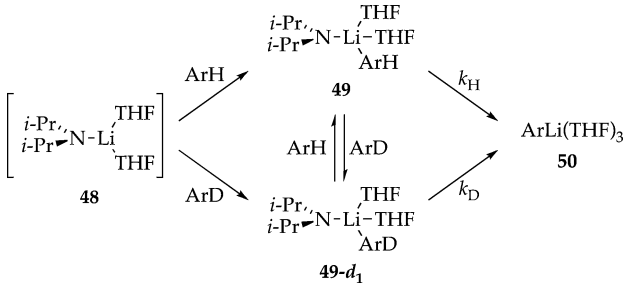

scenario, **49** metalates to give **50** as quickly as it is formed—ArH does not dissociate from **49** nor do **49** and **49-d_1** exchange by any mechanism. The rate law is still described by eq 23, and the metalation rates would depend on both the structure and concentration of ArH. The standard and competitive isotope effects, however, would both be unity ($k_H/k_D = 1$). In a second scenario, a scenario that reflects the experimental observations, formation of **49** is rate limiting but exchange of **49** and **49-d_1** with free arene occurs before proton transfer. Whereas the standard isotope effect would be unity because the proton transfer is post rate limiting, the facile ArH–ArD exchange gives the LDA monomer a choice of which substrate to metalate: the preference for ArH over ArD would be pronounced, making the competitive isotope effect large. If the reaction is followed to full conversion, one would observe biphasic kinetics as observed in Figure 6. This particular scenario has the added constraint that rapid ArH–ArD exchange has to be an associative substitution of the arenes rather than a dissociation to uncomplexed monomer **48**. To assume that **48** and **49** are at equilibrium is tantamount to assuming proton transfer (k_3) is rate limiting, which conflicts with the central tenet of case 2 that complexation is rate limiting.

Case 3: Rate-Limiting Deaggregation. Assuming that deaggregation of dimer **5** to form monomer **48** is rate limiting, the reassociation of two monomers would be slow compared to complexation and all subsequent steps ($k_{-1}[\mathbf{48}]^2 \ll k_2[\mathrm{ArH}][\mathbf{48}]$ and $k_3[\mathbf{49}]$). The rate law would show a first-order dependence on LDA concentration, an order in THF reflecting the number of additional ligands required to deaggregate dimer **5**, and a rate that is independent of the ArH concentration (zeroth order). Whereas the standard isotope effect would be unity, the competitive isotope effect would be large *provided that ArH–ArD exchange on monomer **49** is fast relative to proton transfer.* Unlike the more restrictive case 2, a facile **48**–**49** equilibrium suffices. Case 3 corresponds to an uncatalyzed/unmediated rate-limiting LDA deaggregation, a deaggregation that should occur in LDA/THF solution in the absence of any other species.

Case 4: Partial Rate-Limiting Proton Transfer. This simple example offers an excellent opportunity to illustrate the concept of partial rate limitation. Allusions are made throughout the text to the appearance of upward curvature arising from either catalysis or deuteration (see Figures 5 and 6 for examples). Curvature will appear if a rate-limiting deaggregation (zeroth-order decays; case 3) shifts to a rate-limiting proton transfer (first-order decays; case 1). This shift can occur either by facilitating the reaggregation ($k_{-1}[\mathbf{48}]^2$) or by retarding the proton transfer ($k_3[\mathbf{49}]$). Acceleration of the reaggregation was discussed generically in the context of catalysis and eq 22 and becomes germane to the mixed aggregation effects discussed below. The metalation can be retarded through deuteration via the affiliated large kinetic isotope effect.

We have described very complex behavior—changes in curvatures, reaction orders, and isotope effects—that could stem from a relatively simple mechanism by assuming that deaggregation, complexation, or proton transfer could be rate limiting. Reality may be even more complex. For the time being, readers should ignore the possible intermediacy of the tetramers illustrated in Scheme 1 (we will return to these shortly) and focus on the cascade leading from LDA dimer **5** to monomer **26** (Scheme 2). Recall that the computed activation barriers rise across the sequence with the final deaggregation to form monomer the highest barrier.[12]

What would happen if one of the dimeric intermediates in Scheme 2 could react with ArH? Take, for example, a reaction involving open dimer **29** (Scheme 8). If **29** and corresponding substrate-LDA complex **51** are both formed reversibly, proton

Scheme 8

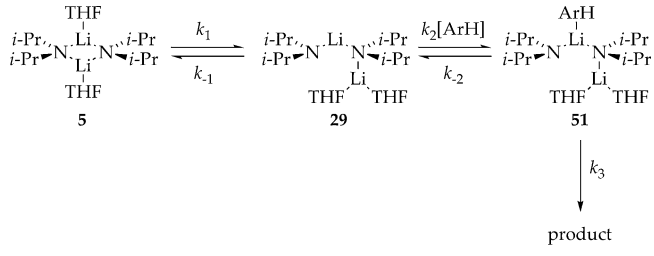

dx.doi.org/10.1021/jo302408r | J. Org. Chem. 2013, 78, 4214–4230

transfer will be rate limiting. Such open-dimer-based reactions are well-precedented.[37] By analogy to the monomer-based metalation in Scheme 5, however, we posit that the rate-limiting step could be complexation or deaggregation. On repeating the very same analysis described by cases 1−4 (above), the reaction orders and kinetic isotope effects (standard and competitive) are predicted to change markedly depending on the relative magnitudes of the rate constants. We need not repeat this analysis here.

Now imagine that *any* of the intermediates in Scheme 2 could be intercepted, depending on the choice of substrate. Because of the rise in the barriers along the cascade, intercepting an early intermediate would, all other parameters being equal, afford observed reaction rates that are higher than if an intermediate later in the cascade is intercepted. Moreover, the observed rates, reaction orders, and kinetic isotope effects would depend on which intermediate is intercepted by substrate and which step—deaggregation, complexation, or proton transfer—is rate limiting. The huge variations in rate behaviors and substrate dependencies could create chaos.

Role of Rate-Limiting Steps: Substrate-Dependent Mechanisms. The evidence collected to date supports this general paradigm. Metalation of carbamate **6** shows a distinct ArH concentration dependence via rate-limiting transition structure, $[A_2S_2(ArH)]^{\ddagger}$, which could correspond to rate-limiting complexation (**43**) or ArH-dependent deaggregation (**44**). Prompted by the studies described in this manuscript, follow-up studies showed that the proton transfer step during the metalation of **6** is post rate limiting, and the analogous deuterium transfer is partially rate limiting.[50] Metalation of arene **10** (eq 4) displays a contrasting zeroth-order dependence on substrate traced to a rate-limiting partial deaggregation via a disolvated-dimer-based transition structure (**13**); complexation and metalation of substrate are post-rate-limiting steps. The large competitive isotope effect indicates that the post-rate-limiting proton transfer is necessarily preceded by a facile ArH−ArD exchange. By slowing the metalation with isotopic labeling, the post-rate-limiting metalation of **10** was shown to involve tetra- and pentasolvated dimers (triple ions **14** and **15**). With the aid of efficient LiCl-catalyzed dimer−monomer exchange that causes a further shift in the rate-limiting step, the critical deprotonation occurs via monomer-based transition structures **16** and **17**.

The notion of several possible rate-limiting deaggregations depending on choice of substrate or conditions is reinforced by comparing previous studies of 1,4-additions of LDA (eq 5). Whereas metalation of arene **10** proceeds via rate-limiting transition structure **13**, 1,4-additions occur via transition structure **20**. The different solvation numbers of **13** and **20** distinguish them as distinctly different rate-limiting deaggregation events. We showed that both react via monomers under LiCl catalysis.

We can now place the metalation of pyridine **1** in context. Standard isotope effects approaching unity for metalations of **1** and **1**-d_1, in conjunction with large competitive isotope effects and biphasic kinetics (Figure 6), offer compelling evidence of a post-rate-limiting proton transfer. The first-order substrate dependence corresponds to either rate-limiting complexation (**43**) or deaggregation (**44**). A large competitive isotope effect and biphasic kinetics (Figure 6) show that facile ArH−ArD exchange (akin to that illustrated in Scheme 7) must occur after the rate-limiting step but before the proton transfer. Although we cannot rigorously exclude substrate complexation to form **49** as rate limiting, we favor rate-limiting deaggregation via **48**.

On the Role of Tetramers. LDA orders in the range of 1.2−1.7 suggest contributions from higher aggregates. What makes these orders so odd is that other reactions involving rate-limiting deaggregations (eqs 3−5) seem to proceed only via dimer-based pathways. We must confess that we still worry that unseen variables in the metalations of **1** are causing mischief, but no amount of experimentation eliminated this inconvenient truth. They are also appearing in ongoing studies of other ortholithiations.

A trimer-based mechanism to explain the high, fractional orders (eqs 8−10) was dismissed for the simple reason that trimer formation seems to require LDA monomer as an intermediate, and monomers were shown to be efficacious intermediates in their own right. Consequently, we turned to a composite mechanism invoking parallel pathways via LDA dimers (eqs 6 and 7) and tetramers (eqs 11 and 12).[39] Spectroscopic and computational studies of tetramer-based aggregate exchanges summarized in Scheme 1 are telling.[12] Moreover, rate studies of LiCl- and ArLi-catalyzed deaggregations implicate mixed tetrameric intermediates (below) as do analogous studies of LDA-lithium enolate condensations.[5b] Thus, the evidence supporting tetrameric intermediates is considerable.

We have two fundamental questions about tetramers for which we can only offer some rather speculative answers:

Could tetramers serve as intermediates en route to monomers? The high energetic cost of deaggregating LDA dimer **5** via transition structure **20** stems, at least in part, from the concurrent formation of *two* high energy species. To use an analogy, this might be akin to a solvolysis that forms a carbocation and an alkoxide. Circumventing the dilemma posed by solvolyses requires stabilizing one of the two fragments, making it a good leaving group. For the dissociation of a tetramer to a trimer and monomer, trimeric ladder **25** assumes the role of leaving group, demanding liberation of only *one* highly destabilized monomer. Further deaggregation of **25** reaps the benefits of a dimer-based leaving group. If tetramers are indeed the intermediates en route to monomers (eq 24), the principle of microscopic reversibility demands that the reaction in reverse, the conversion of monomers to dimers, also proceed via tetramer intermediates.[48] That is an odd concept.

$$2A_2 \rightleftharpoons A_4 \rightleftharpoons A_3 + A \rightleftharpoons A_2 + 2A \qquad (24)$$

Why are LDA tetramers affiliated with the metalation of some but not all substrates? The short answer is that we do not know. A slightly more constructive answer is that the properties that enable fluoropyridines to intercept a particular dimeric intermediate in Scheme 2 might correlate with the properties allowing them to intercept ladders (see **45** or **46**). Further speculation should probably await additional examples.[13,39b−e,51]

LiCl-Catalyzed LDA Deaggregation. The role of LiCl catalysis, both the mechanistic details and the role of catalysis in probing the mechanism of the metalation, demand further consideration. Effects of lithium salts on organolithium structure and reactivity, so-called mixed aggregation effects, are now legion.[52] Mechanistically well-defined examples, however, are quite rare by comparison.[52f] These salt effects are presumed to derive from the direct reaction of mixed aggregates with substrates. The critical assumption is that the LiX salt, whether observably affiliated with the reactant or not,

dx.doi.org/10.1021/jo302408r | J. Org. Chem. 2013, 78, 4214−4230

is intimately involved in the rate- or product-determining transition structure(s). The role of LiCl in LDA/THF-mediated metalations at −78 °C are altogether different. To the best of our knowledge, LiCl-catalyzed deaggregation to monomer is undocumented. It will only be observed for reactions in which deaggregation is either rate limiting or is precluded altogether by a high barrier (forcing reaction out of the aggregated form). No catalysis by LiCl will be observed if all aggregation states fully equilibrate on the time scales of reaction without added catalyst.

Previous studies of ortholithiation[11] foreshadowed *catalysis* by LiCl. Rate studies described herein confirmed a LiCl-catalyzed deaggregation of LDA dimer to monomer. We found a second-order saturation behavior in LiCl (Figure 8) that does *not* derive from Michaelis–Menten kinetics but rather from a shift in the rate-limiting step from LDA deaggregation to proton transfer. The rate studies implicate the fleeting intermediacy of heterotetramers, $A_2(LiCl)_2$. We hasten to add that the resting state of LiCl is a mixture of mixed trimer **32** and dimer **33**; we have minimal insights into the fate of the mixed aggregates during the metalation. In light of the discussion of homotetramer-based intermediates in Scheme 1 and mixed tetramer intermediates from aryllithium catalysis, however, the high order in LiCl seems more than coincidental, suggesting the intermediacy of LDA–LiCl mixed tetramers such as in Scheme 9 (X = Ar).[12,13,53] Alternatively, serial condensation of LDA

Scheme 9

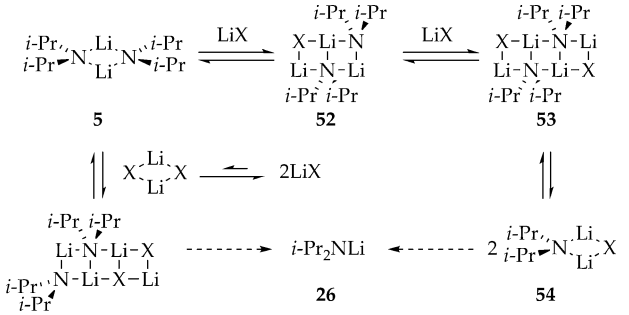

dimer **5** with two LiCl monomers would afford isomeric ladder **53** that could split into mixed dimers and eventually yield monomeric LDA.

As noted previously, chloride ion could also function as a strongly binding THF equivalent to facilitate deaggregation (Scheme 10).[5c] The intermediacy of complex ion **55** is consistent with both the high LiCl order and positive order in THF. The cationic triple ion fragment (Li–Cl–Li),[54] the chloride adduct of a lithium amide open dimer,[55] and transition structure **56** bearing a bridging THF ligand have computational and experimental support.[56]

Although the mechanistic details of the catalysis are both complex and interesting in their own right, the role that such catalysis played in probing the mechanism is especially important. Recall from the tutorial on rate limitation that catalyzing the *reaggregation* elicits a shift in the rate-limiting step (Scheme 5). Rate studies show that catalyzing the dimer–monomer preequilibrium shifts the rate-limiting step from deaggregation of dimer **5** to monomer-based proton transfer, which allowed us to examine some details beyond the deaggregation. We hasten to add, however, that monomer-based metalations *with* catalysis do not necessarily implicate

Scheme 10

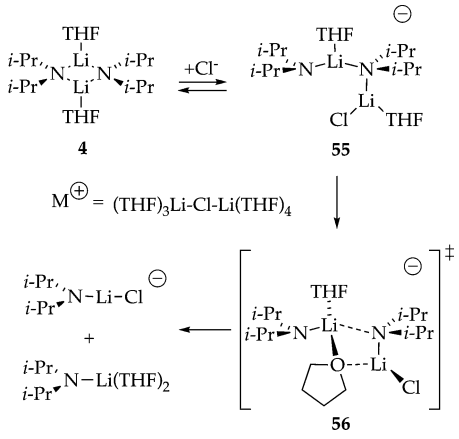

monomer-based metalations in a post-rate-limiting metalation *without* catalysis.

Autocatalysis. Catalysis by aryllithium **3**, so-called autocatalysis, shows strong parallels with the catalysis by LiCl. The role of mixed tetramers (Schemes 9 or 10) is gleaned from both *second-order* saturation behavior (Figure 12) as well as from the method of continuous variations[45,46] (the Job plot in Figure 11). The maximum at equal parts LDA and ArLi and curvatures in Figures 11 and 12 strongly support a 2:2 stoichiometry. Autocatalysis previously observed for metalations of fluorocarbamates (eq 3) differ in two respects: (1) autocatalysis of the carbamate metalation appears to occur via a mixed-dimer-based transition structure, $[A(ArLi)]^{‡}$, rather than via mixed tetramers, and (2) LDA–ArLi mixed dimers are observable for carbamate-derived aryllithiums whereas no mixed aggregates of any kind are observed for pyridyllithium **3**.

Lingering Issues. We sought evidence that the miniscule nonzero intercept in Figure 2 corresponds to a rate-limiting deaggregation in which substrate plays no role whatsoever. In principle, all LDA-mediated reactions that share a common rate-limiting deaggregation would necessarily share common transition structures and reaction rates. This notion is supported by similar rates observed at ultra low concentrations of **1**, **1**-d_1, **2**, and **2**-d_2[57] as well as similar rates for several arene ortholithiations[5] and LDA-mediated 1,4-additions.[5b] The intervention of a putative tetramer-based pathway, however, even at ultra low substrate concentration, precludes a simple analysis.

The implication of tetramers—homotetrameric LDA as well as LDA–LiCl and LDA–ArLi mixed tetramers—displays a substrate specificity suggesting that only some substrates can trap fleeting tetrameric intermediates. Failed attempts to mimic the catalysis by adding **34**–**37**, however, underscore an inability to identify some special structural feature of fluoropyridines. Limited evidence that difluoropyridine **2** is more efficient than **1** at mediating the rate-limiting deaggregation simply adds to the mystery of how substrates assist deaggregations.

Despite evidence that different substrates can intercept different intermediates along the dimer–monomer and dimer–tetramer cascades, we suspect that the chemistry may funnel through LDA monomers in many instances with only substrate-dependent rate-limiting steps varying. The evidence that LiCl and ArLi accelerate the reaction by catalyzing the LDA dimer–monomer equilibration is compelling. Whereas the case for *uncatalyzed* monomer-based 1,4-additions (eq 5) is also

dx.doi.org/10.1021/jo302408r | J. Org. Chem. 2013, 78, 4214–4230

compelling, the evidence of monomer-based intermediates in the *uncatalyzed* metalation of **1** is strong but still circumstantial.

It is clear that different lithium salts display markedly varying capacities to elicit accelerations of LDA-mediated reactions by catalyzing the deaggregation. We have made progress toward understanding the dynamics of LDA aggregate exchanges in THF. However, the mechanisms of deaggregation and aggregate−aggregate exchange for LDA dimer **5** and LDA−LiX mixed aggregates remain poorly defined and likely to be revealed only reluctantly.

CONCLUSIONS

For years, we studied LDA-mediated reactions between −55 and 0 °C. At these temperatures, all aggregation and solvation events are rapid relative to reactions with substrates. It is now clear that LDA dimer **5** deaggregates and exchanges with LiX aggregates with half-lives of many minutes in THF at −78 °C. Consequently, any reaction of LDA that proceeds at measurable rates in THF at −78 °C is likely to be influenced by the rates at which aggregates exchange. Such rate-limiting aggregation events prove highly susceptible to autocatalysis as well as to catalysis by added lithium salts.

Lithiations of 2-fluoropyridines described herein are probably the most vexing reported to date, but a coherent mechanistic paradigm is emerging. Progress is incremental largely because of our profoundly limited understanding of *how* organolithium aggregates exchange. The notion that two substrates can react via rate-limiting deaggregations in which the critical deaggregation steps are *different* is odd. Evidence is also mounting that different transient aggregates of LDA can be intercepted depending on the precise structure of the substrate. Moreover, evidence is mounting that LDA monomers can form not only via both direct deaggregation of dimers but also via homo- and mixed-aggregated *tetramers*, a conclusion we draw with some trepidation. We will be watching for additional support as studies continue.

In closing, we ask a simple question: Are the efforts to untangle this mess justifiable? We believe the answer is yes. Of practical importance, commercial LDA is free of LiCl, whereas LDA generated in situ from *n*-BuLi contains sufficient LiCl to catalyze deaggregation. The relative reactivities of the two forms of LDA can vary by as much as 10^3. At a more academic level, the rate-limiting aggregation events observed for LDA/THF are offering what may be a unique window into the details of aggregate exchanges. And, of course, LDA is one of the most commonly used reagents, suggested by one extensive survey to be *the* most commonly used reagent,[58] in organic synthesis. It seems self-evident that understanding its chemistry is worthy of considerable effort.

EXPERIMENTAL SECTION

Reagents and Solvents. THF and hexanes were distilled from blue or purple solutions containing sodium benzophenone ketyl. The hexane contained 1% tetraglyme to dissolve the ketyl. LiCl-free LDA was prepared and multiply recrystallized as described previously.[5b] Solutions of LDA were titrated using a literature method.[59] Arenes **1** and **2** are commercially available. Deuterated analogues were prepared as described below. Et_3N·HCl was recrystallized from THF/2−propanol. Compound **37** is known.[60]

3-Deutero-2-fluoropyridine. A 1.6 M solution of *n*-butyllithium (22.2 mL, 35.6 mmol) in hexanes was added via syringe to a solution of dry diisopropylamine (5.0 mL, 3.61 g, 35.6 mmol) in dry THF at −78 °C under argon. After the solution was stirred for 20 min, 1.0 equiv of 2-fluoropyridine (3.0 mL) was added to the LDA solution. The solution was stirred at −78 °C for 1.0 h, after which 1.0 equiv of *n*-butyllithium was added to the solution via syringe and the reaction was quenched with a THF/D_2O (10:1, 10 mL) after 15−20 min of stirring. The organic layer was washed with aqueous NaCl (3 × 10 mL), dried over Na_2SO_4 and filtered. Distillation and flash chromatography (pentane/ether) afforded 3−deutero−2−fluoropyridine (2.4 g, 27.6 mmol) as a colorless liquid in 80% yield and 98% deuteration as shown by ^{1}H NMR spectroscopy.

2-Fluoro-4-(trimethylsilyl)pyridine (36). A 1.3 M solution of *i*-PrMgCl·LiCl[61] (31.5 mL, 40.9 mmol) in THF was added via syringe to a solution of commercially available 4-bromo-2-fluoropyridine (6.0 g, 34.1 mmol) in dry THF (25 mL) at 0 °C under Ar. After the completion of Br/Mg exchange (checked by GC analysis of quenched reaction aliquots), the supernatant obtained from centrifuging ∼3 equiv of 3:1 Me_3SiCl/Et_3N was added to the solution, and the solution was stirred at rt for ∼15 h. The reaction was quenched with water and the organic layer was washed with aqueous NaCl (3 × 10 mL), dried over Na_2SO_4, filtered, and evaporated to dryness under reduced pressure. Distillation under reduced pressure followed by flash chromatography (pentane/ether) afforded 2-fluoro-4-(trimethylsilyl)-pyridine (5.2 g, 30.7 mmol) as a colorless liquid in 90% yield: ^{1}H NMR ($CDCl_3$) δ 8.14 (dt, J = 4.8, 0.9 Hz, 1H), 7.22 (m, 1H), 6.99 (m, 1H), 0.27 (s, 9H). Inset shows the peaks in the aromatic region; ^{13}C NMR ($CDCl_3$) δ 163.5 (d, J = 242.3 Hz), 157.7 (d, J = 4.9 Hz), 146.8 (d, J = 12.9 Hz), 125.5 (d, J = 4.0 Hz), 113.9 (d, J = 33.6 Hz), −1.6 (s). HRMS ($C_8H_{11}NFSi$, double-focusing sector mass analyzer with 70 eV electron impact ionization) requires m/z 169.0723, found 169.0727.

IR Spectroscopic Analyses. IR spectra were recorded using an in situ IR spectrometer fitted with a 30-bounce, silicon-tipped probe. The spectra were acquired in 16 scans at a gain of 1 and a resolution of 4 cm^{-1}. A representative reaction was carried out as follows: The IR probe was inserted through a nylon adapter and an O-ring seal into an oven-dried, cylindrical flask fitted with a magnetic stir bar and a T-joint. The T-joint was capped with a septum for injections and a nitrogen line. After evacuation under full vacuum, heating, and flushing with nitrogen, the flask was charged with LDA (107 mg, 1.00 mmol) in THF (9.9 mL) and cooled in a dry ice−acetone bath prepared from fresh acetone. After recording a background spectrum, arene **1** (100 μL) was added with stirring. IR spectra were recorded at 30-s intervals over the course of the reaction. Absorbances corresponding to the arene moieties were monitored.

NMR Spectroscopic Analyses. All NMR tubes were prepared using stock solutions and sealed under partial vacuum. Standard ^{6}Li, ^{13}C, and ^{19}F NMR spectra were recorded on a 500 MHz spectrometer at 73.57, 125.79, 50.66, and 470.35 MHz (respectively). The ^{6}Li, ^{13}C, ^{15}N, and ^{19}F resonances are referenced to 0.30 M [^{6}Li]LiCl/MeOH at −90 °C (0.0 ppm), the CH_2O resonance of THF at −90 °C (67.57 ppm), neat Me_2NEt at −90 °C (25.76 ppm), and C_6H_5F in neat THF at −78 °C (−113.15 ppm), respectively.

Rate Studies Using ^{19}F NMR Spectroscopy. The rates of metalation were monitored using ^{19}F NMR spectroscopy on a 500 MHz spectrometer at 470.35 MHz. Isotopic perturbation is sufficient to resolve the resonances of **1**, **2**, **3** and **4** by ^{19}F NMR spectroscopy. Spectroscopic samples were prepared by injecting 100 μL of fluoropyridine via 25 μm i.d. flexible capillary tubing by gastight syringe directly into the solution of LDA (500 μL) at −78 °C in the NMR probe. The LDA solution is allowed to cool at −78 °C for couple of minutes prior to injecting the substrate solution. Previous studies have shown that the temperature equilibration occurs in <30 s after the addition of substrate.[5a] $T1$ relaxation times were determined for all species, and the delay between scans was set to >5 × $T1$ to ensure accurate integrations.

Computations. DFT computations were optimized at the B3LYP/6-31G(d) level[20] with single-point calculations at the MP2 level of theory. Saddle points were verified by a single negative frequency.

dx.doi.org/10.1021/jo302408r | J. Org. Chem. 2013, 78, 4214−4230

■ ASSOCIATED CONTENT

Supporting Information

Spectroscopic data, rate data, select experimental procedures, and complete ref 21. This material is available free of charge via the Internet at http://pubs.acs.org.

■ AUTHOR INFORMATION

Corresponding Author

*E-mail: dbc6@cornell.edu.

Notes

The authors declare no competing financial interest.

■ ACKNOWLEDGMENTS

We thank the National Institutes of Health (GM39764) for direct support of this work. We thank Meredith Palmer for assistance with the cover design.

■ REFERENCES

(1) (a) Schlosser, M. *Angew. Chem., Int. Ed.* **2005**, *44*, 376. (b) Schlosser, M.; Rausis, T. *Eur. J. Org. Chem.* **2004**, 1018. (c) Kuethe, J. T.; et al. *Tetrahedron* **2009**, *65*, 5013. (d) Güngör, T.; Marsais, F.; Quéguiner, G. *J. Organomet. Chem.* **1981**, *215*, 139.

(2) (a) Quéguiner, G.; Marsais, F.; Snieckus; Epsztajn, J. *Adv. Heterocycl. Chem.* **1991**, *52*, 187. (b) Mongin, F.; Quéguiner, G. *Tetrahedron* **2001**, *57*, 5897. (c) Mongin, F.; Quéguiner, G. *Tetrahedron* **2001**, *57*, 4059. (d) Merino, P. *Prog. Heterocycl. Chem.* **1999**, *11*, 21. (e) Clayden, J. In *The Chemistry of Organolithium Compounds*; Rappoport, Z., Marek, I., Eds.; Wiley: New York, 2004; Vol. *1*, p 495. (f) Caubere, P. In *Reviews of Heteroatom Chemistry*; MYU: Tokyo, 1991; Vol. *4*, pp 78−139. (g) Caubere, P. *Chem. Rev.* **1993**, *93*, 2317. (h) Marsais, F.; Quéguiner, G. *Tetrahedron* **1983**, *39*, 2009. (i) Collins, I. *Perkin 1* **2000**, 2845. (j) Schlosser, M.; Mongin, F. *Chem. Soc. Rev.* **2007**, *36*, 1161. (k) Hartung, C. G.; Snieckus, V. In *Modern Arene Chemistry*; Astruc, D., Ed.; Wiley-VCH: Weinheim, 2002; Chapter 10. (l) Snieckus, V. *Chem. Rev.* **1990**, *90*, 879. (m) Taylor, C. M.; Watson, A. J. *Curr. Org. Chem.* **2004**, *8*, 623. (n) Bakker, W. I. I.; Wong, P. L.; Snieckus, V. Lithium Diisopropylamide. In *e-EROS Encyclopedia of Reagents for Organic Synthesis*; Paquette, L. A., Ed.; John Wiley: New York, 2001.

(3) (a) Fort, Y. 2-Fluoropyridine. In *e-EROS Encyclopedia of Reagents for Organic Synthesis*; John Wiley & Sons: NewYork, 2001. (b) Bhardwaj, P.; Forgione, P. 2,6-Difluoropyridine. In *e-EROS Encyclopedia of Reagents for Organic Synthesis*; John Wiley & Sons: NewYork, 2001.

(4) (a) Eames, J. Product Subclass 6: Lithium Amides. In *Science of Synthesis*; Snieckus, V., Ed.; Thieme: New York, 2006; Vol. *8a*, p 173. (b) Clayden, J. *Organolithiums: Selectivity for Synthesis*; Pergamon: New York, 2002.

(5) (a) Singh, K. J.; Hoepker, A. C.; Collum, D. B. *J. Am. Chem. Soc.* **2008**, *130*, 18008. (b) Ma, Y.; Hoepker, A. C.; Gupta, L.; Faggin, M. F.; Collum, D. B. *J. Am. Chem. Soc.* **2010**, *132*, 15610. (c) Hoepker, A. C.; Gupta, L.; Ma, Y.; Faggin, M. F.; Collum, D. B. *J. Am. Chem. Soc.* **2011**, *133*, 7135.

(6) For examples of reactions that are fast relative to the rates of aggregate−aggregate exchanges, see: (a) McGarrity, J. F.; Ogle, C. A. *J. Am. Chem. Soc.* **1985**, *107*, 1810. (b) Jones, A. C.; Sanders, A. W.; Bevan, M. J.; Reich, H. J. *J. Am. Chem. Soc.* **2007**, *129*, 3492. (c) Thompson, A.; Corley, E. G.; Huntington, M. F.; Grabowski, E. J. J.; Remenar, J. F.; Collum, D. B. *J. Am. Chem. Soc.* **1998**, *120*, 2028. (d) Jones, A. C.; Sanders, A. W.; Sikorski, W. H.; Jansen, K. L.; Reich, H. J. *J. Am. Chem. Soc.* **2008**, *130*, 6060. (e) Kolonko, K. J.; Wherritt, D. J.; Reich, H. J. *J. Am. Chem. Soc.* **2011**, *133*, 16774. (f) See ref 5.

(7) Collum, D. B.; McNeil, A. J.; Ramirez, A. *Angew. Chem., Int. Ed.* **2007**, *46*, 3002.

(8) Liao, S.; Collum, D. B. *J. Am. Chem. Soc.* **2003**, *125*, 15114.

(9) (a) Espenson, J. H. *Chemical Kinetics and Reaction Mechanisms*, 2nd ed.; McGraw−Hill: New York, 1995; Chapter 2, p 44. Atkins, P. W.; Jones, L. L. *Chemical Principles: the Quest for Insight*, 2nd ed.; W H. Freeman: New York, 2002.

(10) (a) Besson, C.; Finney, E. E.; Finke, R. G. *J. Am. Chem. Soc.* **2005**, *127*, 8179. (b) Besson, C.; Finney, E. E.; Finke, R. G. *Chem. Mater.* **2005**, *17*, 4925. (c) Huang, K. T.; Keszler, A.; Patel, N.; Patel, R. P.; Gladwin, M. T.; Kim-Shapiro, D. B.; Hogg, N. *J. Biol. Chem.* **2005**, *280*, 31126. (d) Huang, Z.; Shiva, S.; Kim-Shapiro, D. B.; Patel, R. P.; Ringwood, L. A.; Irby, C. E.; Huang, K. T.; Ho, C.; Hogg, N.; Schechter, A. N.; Gladwin, M. T. *J. Clin. Invest.* **2005**, *115*, 2099. (e) Tanj, S.; Ohno, A.; Sato, I.; Soai, K. *Org. Lett.* **2001**, *3*, 287. (f) Barrios-Kabderism, F.; Carrow, B. P.; Hartwig, J. F. *J. Am. Chem. Soc.* **2008**, *130*, 5842.

(11) Gupta, L.; Hoepker, A. C.; Singh, K. J.; Collum, D. B. *J. Org. Chem.* **2009**, *74*, 2231.

(12) Hoepker, A. C.; Collum, D. B. *J. Org. Chem.* **2011**, *75*, 7985.

(13) (a) Gregory, K.; Schleyer, P. v. R.; Snaith, R. *Adv. Inorg. Chem.* **1991**, *37*, 47. (b) Mulvey, R. E. *Chem. Soc. Rev.* **1991**, *20*, 167. (c) Beswick, M. A.; Wright, D. S. In *Comprehensive Organometallic Chemistry II*; Abels, E. W., Stone, F. G. A., Wilkinson, G., Eds.; Pergamon: New York, 1995; Vol. *1*, Chapter 1. (d) Mulvey, R. E. *Chem. Soc. Rev.* **1998**, *27*, 339.

(14) Review of ^{6}Li NMR spectroscopy: Günther, H. *J. Brazil. Chem.* **1999**, *10*, 241.

(15) Collum, D. B. *Acc. Chem. Res.* **1993**, *26*, 227.

(16) Warming pyridyllithium **4** causes reversible protonation by *i*-Pr_2NH and subsequent 1,2-addition to form the corresponding 2-aminopyridine: Viciu, M.; Gupta, L.; Collum, D. B. *J. Am. Chem. Soc.* **2010**, *132*, 6361.

(17) Similar $^{2}J_{C-F}$ values have been observed for related 2-fluorophenyllithiums: (a) Singh, K. J.; Collum, D. B. *J. Am. Chem. Soc.* **2006**, *128*, 13753. (b) Menzel, K.; Fisher, E. L.; DiMichele, L.; Frantz, D. E.; Nelson, T. D.; Kress, M. H. *J. Org. Chem.* **2006**, *71*, 2188. (c) See ref 43a,b.

(18) $^{2}J_{C-F}$ values have been correlated with π-bond orders and total electronic charge at the ^{13}C atom: (a) Doddrell, D.; Jordan, D.; Riggs, N. V. *J. Chem. Soc., Chem. Commun.* **1972**, 1158. (b) Doddrell, D.; Barfield, M.; Adcock, W.; Aurangzeb, M.; Jordan, D. *J. Chem. Soc., Perkin Trans. 2* **1976**, 402.

(19) For reviews of structural studies using ^{19}F NMR spectroscopy, see: (a) Gakh, Y. G.; Gakh, A. A.; Gronenborn, A. M. *Magn. Reson. Chem.* **2000**, *38*, 551. (b) McGill, C. A.; Nordon, A.; Littlejohn, D. *J. Process Anal. Chem.* **2001**, *6*, 36. (c) Espinet, P.; Albeniz, A. C.; Casares, J. A.; Martinez-Ilarduya, J. M. *Coord. Chem. Rev.* **2008**, *252*, 2180.

(20) Frisch, M. J. et al. *GaussianVersion 3.09*; revision A.1; Gaussian, Inc.: Wallingford, CT, 2009.

(21) Derivations and experimental details are included in the Supporting Information.

(22) (a) Kottke, T.; Sung, K.; Lagow, R. J. *Angew. Chem., Int. Ed. Engl.* **1995**, *34*, 1517. (b) Reich, H. J.; Green, D. P.; Medina, M. A.; Goldenberg, W. S.; Gudmundsson, B. Ö.; Dykstra, R. R.; Phillips, N. H. *J. Am. Chem. Soc.* **1998**, *120*, 7201. (c) Bonasia, P. J.; Arnold, J. *J. Organomet. Chem.* **1993**, *449*, 147.

(23) (a) Reich, H. J.; Borst, J. P.; Dykstra, R. R.; Green, D. P. *J. Am. Chem. Soc.* **1993**, *115*, 8728. (b) Wong, M. K.; Popov, A. I. *J. Inorg. Nucl. Chem.* **1972**, *34*, 3615. (c) Yakimansky, A. V.; Müller, A. H.; Beylen, M. V. *Macromolecules* **2000**, *33*, 5686. (d) Goralski, P.; Chabanel, M. *Inorg. Chem.* **1987**, *26*, 2169 and references cited therein.

(24) (a) Kottke, T.; Stalke, D. *Angew. Chem., Int. Ed. Engl.* **1993**, *32*, 580. (b) Rennels, R. A.; Maliakal, A. J.; Collum, D. B. *J. Am. Chem. Soc.* **1998**, *120*, 421.

(25) Evans, A., *Potentiometry and Ion-Selective Electrodes*; Wiley: New York, 1987.

(26) Fuji, T. *Anal. Chem.* **1992**, *64*, 775.

(27) (a) Marck, W.; Huisgen, R. *Chem. Ber.* **1960**, *93*, 608. (b) Gaudemar-Bardone, F.; Gaudemar, M. *Synthesis* **1979**, 463. (c) Reetz, M. T.; Maier, W. F. *Liebigs Ann. Chem.* **1980**, 1471.

(d) Williard, P. G.; Carpenter, G. B. *J. Am. Chem. Soc.* **1986**, *108*, 462. (f) Williard, P. G.; Salvino, J. M. *J. Org. Chem.* **1993**, *58*, 1. (e) Morrison, R. C.; Hall, R. W.; Rathman, T. L. Stable Lithium Diisopropylamide and Method of Preparation. U.S. Patent 4,595,779, June 17, 1986.

(28) Traces of oxygen, air, water, and joint greases failed to elicit unusual rate effects.

(29) Snaith and co-workers underscored the merits of R_3NHX salts as precursors to anhydrous LiX salts: Barr, D.; Snaith, R.; Wright, D. S.; Mulvey, R. E.; Wade, K. *J. Am. Chem. Soc.* **1987**, *109*, 7891.

(30) Zhao, P.; Collum, D. B. *J. Am. Chem. Soc.* **2003**, *125*, 14411 and references cited therein.

(31) Rein, A. J.; Donahue, S. M.; Pavlosky, M. A. *Curr. Opin. Drug Discovery Dev.* **2000**, *3*, 734.

(32) (a) Espenson, J. H. *Chemical Kinetics and Reaction Mechanisms*, 2nd ed.; McGraw-Hill: New York, 1995. (b) Rae, M.; Berberan-Santos, M. N. *J. Chem. Educ.* **2004**, *81*, 436.

(33) Determining initial rates (slopes) of a curved decay can be strongly dependent on the percent conversion, requiring a compromise between adequate sample size and loss of linearity. This problem is avoided by fitting a significant part of the decay, a portion that includes some curvature, to a third-order polynomial ($at^2 + bt + c$). Be sure not to include too much curvature or the function will no longer fit well. The parameter b represents the rate at time = zero. (One may verify this by taking the first derivative with respect to t and setting $t = 0$. Initial rate = $f'(0) = b$.) The experimental observable (NMR intensity, IR absorbance, etc.) to concentration allows valid comparison between initial rates of varying concentrations and/or experimental conditions.

(34) The concentration of LDA, although expressed in units of molarity, refers to the concentration of the monomer unit (normality). The concentration of THF is expressed as total concentration of free (uncoordinated) ligand.

(35) Superposition of autocatalysis on a first-order decay can produce a perfectly linear decay (ref 5a).

(36) Ma, Y.; Collum, D. B. *J. Am. Chem. Soc.* **2007**, *129*, 14818 and references cited therein.

(37) For leading references to spectroscopic, crystallographic, and kinetic evidence of open dimers, see: Ramirez, A.; Sun, X.; Collum, D. B. *J. Am. Chem. Soc.* **2006**, *128*, 10326.

(38) Cyclic tetramers of lithium 2,2,6,6-tetramethylpiperidide were shown to react by dissociation to dimers: Wiedemann, S. H.; Ramírez, A.; Collum, D. B. *J. Am. Chem. Soc.* **2003**, *125*, 15893.

(39) Lithium amide tetramers: (a) Cyclic: Lucht, B. L.; Collum, D. B. *J. Am. Chem. Soc.* **1994**, *116*, 7949. (b) Ladders: Armstrong, D. R.; Barr, D.; Clegg, W.; Mulvey, R. E.; Reed, D.; Snaith, R.; Wade, K. *J. Chem. Soc., Chem. Commun.* **1986**, 869. (c) Ladders: Gardiner, M. G.; Raston, C. L. *Inorg. Chem.* **1996**, *35*, 4047. (d) Ladders: Vestergren, M.; Eriksson, J.; Hilmersson, G.; Hakansson, M. *J. Organomet. Chem.* **2003**, *682*, 172. (e) Ladders: Boche, G.; Langlotz, I.; Marsch, M.; Harms, K.; Nudelman, N. E. S. *Angew. Chem.* **1992**, *104*, 1239. (f) Cubic: Gardiner, M. G.; Raston, C. L. *Inorg. Chem.* **1995**, *34*, 4206.

(40) Competitive and intramolecular isotope effects can be used to examine postrate-limiting proton transfer. They differ in that the intramolecular isotope effect demands a symmetry-equivalent choice of H versus D within the same molecule whereas the competitive isotope effect requires an exchange mechanism to establish the choice of H versus D.

(41) (a) Hindermann, D. K.; Cornwell, C. D. *J. Chem. Phys.* **1968**, *48*, 4148. (b) Forsyth, D. A.; Yang, J.-R. *J. Am. Chem. Soc.* **1986**, *108*, 2157. (c) Lambert, J. B.; Greifenstein, L. G. *J. Am. Chem. Soc.* **1973**, *95*, 6150.

(42) (a) Carpenter, B. K., *Determination of Organic Reaction Mechanisms*; Wiley: New York, 1984. (b) Whisler, M. C.; MacNeil, S.; Snieckus, V.; Beak, P. *Angew. Chem., Int. Ed.* **2004**, *43*, 2206.

(43) (a) Chadwick, S. T.; Rennels, R. A.; Rutherford, J. L.; Collum, D. B. *J. Am. Chem. Soc.* **2000**, *122*, 8640. (b) Riggs, J. C.; Ramirez, A.; Cremeens, M. E.; Bashore, C. G.; Candler, J.; Wirtz, M. C.; Coe, J. W.; Collum, D. B. *J. Am. Chem. Soc.* **2008**, *130*, 3406.

(44) Selected examples of fully characterized through-space Li–F interactions: (a) Armstrong, D. R.; Khandelwal, A. H.; Kerr, L. C.; Peasey, S.; Raithby, P. R.; Shields, G. P.; Snaith, R.; Wright, D. S. *Chem. Commun.* **1998**, 1011. (b) Plenio, H.; Diodone, R. *J. Am. Chem. Soc.* **1996**, *118*, 356. (c) Henderson, K. W.; Dorigo, A. E.; Liu, Q.-Y.; Williard, P. G. *J. Am. Chem. Soc.* **1997**, *119*, 11855. (d) Kessar, S. V.; Singh, P.; Singh., K. N.; Bharatam, P. V.; Sharma, A. K.; Lata, S.; Kaur, A. *Angew. Chem., Int. Ed.* **2008**, *47*, 4703. (e) Lee, W.-Y.; Liang, L.-C. *Inorg. Chem.* **2008**, *47*, 3298. (f) Stalke, D.; Klingebiel, U.; Sheldrick, G. M. *Chem. Ber.* **1988**, *121*, 1457. (g) Sini, G.; Tessier, A.; Pytkowicz, J.; Brigaud, T. *Chem.—Eur. J.* **2008**, *14*, 3363 and references cited therein.

(45) (a) Huang, C. Y. *Method Enzymol.* **1982**, *87*, 509. (b) Hirose, K. *J. Inclusion Phenom.* **2001**, *39*, 193. (c) Likussar, W.; Boltz, D. F. *Anal. Chem.* **1971**, *43*, 1265. (d) Olson, E. J.; Bühlmann, P. *J. Org. Chem.* **2011**, *76*, 8406.

(46) Job, P. *Ann. Chim.* **1928**, *9*, 113.

(47) More precisely, introducing catalysis would elevate the rate constant for conversion of SM to I according to $k_{obsd} = k_1 + k_{cat}$.

(48) The principle of microscopic reversibility seems to have been the source of frequent controversies and must be applied with caution. It is not obvious to us, for example, that the following authors, all warning of the risks, would agree with each other's assertions: (a) Blackmond, D. G. *Angew. Chem., Int. Ed.* **2009**, *48*, 2648. (b) Krupka, R. M.; Kaplan, H.; Laidler, K. J. *J. Chem. Soc., Faraday Trans.* **1966**, *62*, 2754. (c) Chandrasekhar, S. *Res. Chem. Intermed.* **1992**, *17*, 173. (d) Burwell, R. L.; Pearson, R. G. *J. Phys. Chem.* **1966**, *70*, 300.

(49) (a) Anderson, D. R.; Faibish, N. C.; Beak, P. *J. Am. Chem. Soc.* **1999**, *121*, 7553. (b) Meyers, A. I.; Mihelich, E. D. *J. Org. Chem.* **1975**, *40*, 3158. (c) Sun, X.; Collum, D. B. *J. Am. Chem. Soc.* **2000**, *122*, 2452. (d) See ref 37 and 43a.

(50) The metalations of carbamate **6** (eq 2) showed an approximate first-order dependence on **6** affiliated with a standard isotope effect that was small (k_H/k_D = 3–4) when compared with some LDA-mediated metalations but still reasonable for a rate-limiting proton transfer. Prompted by the substrate orders and isotope effects described herein, we have reinvestigated the metalation of **6** by monitoring the *competitive* isotope effect and found a large KIE (k_H/k_D > 30) and clear biphasic kinetics. We conclude, therefore, that the proton transfer is only partially rate limiting for **6-*d*$_1$**.

(51) For crystallographically characterized examples of lithium amide ladder structures showing open-dimer-like subunits, see: Armstrong, D. R.; Barr, D.; Clegg, W.; Hodgson, S. M.; Mulvey, R. E.; Reed, D.; Snaith, R.; Wright, D. S. *J. Am. Chem. Soc.* **1989**, *111*, 4719.

(52) For leading references and discussions of mixed aggregation effects, see: (a) Seebach, D. *Angew. Chem., Int. Ed. Engl.* **1988**, *27*, 1624. (b) Seebach, D. In *Proceedings of the Robert A. Welch Foundation Conferences on Chemistry and Biochemistry*; Wiley: New York, 1984; p 93. (c) Tchoubar, B.; Loupy, A. *Salt Effects in Organic and Organometallic Chemistry*; VCH: New York, 1992; Chapters 4, 5, and 7. (d) See also ref 37.

(53) A four-rung LDA/LiX ladder has been characterized: Williard, P. G.; Hintze, M. J. *J. Am. Chem. Soc.* **1987**, *109*, 5539.

(54) (a) Evans, W. J.; Broomhall-Dillard, R. N. R.; Ziller, J. W. *J. Organomet. Chem.* **1998**, *569*, 89. (b) Klingebiel, U.; Tecklenburg, B.; Noltemeyer, M.; Schmidt-Baese, D.; Herbst-Irmer, R. *Z. Naturforsch., B: Chem. Sci.* **1998**, *53*, 355.

(55) Romesberg, F. E.; Collum, D. B. *J. Am. Chem. Soc.* **1994**, *116*, 9198.

(56) Examples and leading references to complex ion pairs, see: Kolonko, K. J.; Biddle, M. M.; Guzei, I. A.; Reich, H. J. *J. Am. Chem. Soc.* **2009**, *131*, 11525.

(57) *Y*-intercepts derived from plots of initial rates versus arene concentration using 0.10 M LDA in neat THF ($M \cdot s^{-1}$) are as follows: **1**, 1.0×10^{-6}; **1-*d*$_1$**, 0.5×10^{-6}; **2**, 3.0×10^{-6}; **2-*d*$_2$**, 0.8×10^{-6}.

(58) A survey of approximately 500 total syntheses compiled by Reich and co-workers revealed LDA to be the most commonly used reagent (personal communication).

(59) Kofron, W. G.; Baclawski, L. M. *J. Org. Chem.* **1976**, *41*, 1879.
(60) Pierrat, P.; Gros, P.; Fort, Y. *Org. Lett.* **2005**, *7*, 697.
(61) Krasovskiy, A.; Knochel, P. *Angew. Chem., Int. Ed.* **2004**, *43*, 3333.